

# Pattern Synthesis via Complex-Coefficient Weight Vector Orthogonal Decomposition

Xue Shi

**Abstract**—This paper presents a new array response control scheme named complex-coefficient weight vector orthogonal decomposition ( $C^2$ -WORD) and its application to pattern synthesis. The proposed  $C^2$ -WORD algorithm is a modified version of the existing WORD approach. We extend WORD by allowing a complex-valued combining coefficient in  $C^2$ -WORD, and find the optimal combining coefficient by maximizing white noise gain (WNG). Our algorithm offers a closed-form expression to precisely control the array response level of a given point starting from an arbitrarily-specified weight vector. In addition, it results less pattern variations on the uncontrolled angles. Elaborate analysis shows that the proposed  $C^2$ -WORD scheme performs at least as good as the state-of-the-art  $A^2$ RC or WORD approach. By applying  $C^2$ -WORD successively, we present a flexible and effective approach to pattern synthesis. Numerical examples are provided to demonstrate the flexibility and effectiveness of  $C^2$ -WORD in array response control as well as pattern synthesis.

**Index Terms**—Array pattern synthesis, array response control, white noise gain, array signal processing.

## I. INTRODUCTION

ARRAY antenna has found numerous applications to radar, navigation and wireless communication. Determining the complex weights for array elements to achieve a desired beam pattern, i.e., array pattern synthesis, is a fundamental problem [1]–[5]. For instance, in radar systems, it is desirable to mitigate returns from interfering signals by designing a pattern with several nulls at specified directions. In some communication systems, it is often required to shape multiple-beam patterns for multi-user reception. Additionally, synthesizing a pattern with broad mainlobe can extend monitoring areas in satellite remote sensing.

With regard to the problem of pattern synthesis, it is expected to control the sidelobe of array response to achieve a pencil beam pattern or to realize a shaped beam pattern complying to a given mask. Quite a number of approaches to pattern synthesis have been reported during the past several decades. For example, given the mainlobe width, Dolph provided an analytical solution to obtain a pattern with minimum uniform sidelobe level [6]. However, this method is only suitable for arrays with particular geometries. For arbitrary arrays, the global search approaches, such as genetic algorithm (GA) [7], particle swarm optimization (PSO) [8] and simulated annealing (SA) [9], are adopted to find the qualified weights yielding satisfactory beam patterns. Nevertheless, the prohibitive amount of computation time limits their practical

use. Adaptive array theory [10] has been utilized in [11]–[13] to synthesize desirable patterns. For this kind of method, the array response levels are adjusted by assigning virtual interferences. Note that the interference-to-noise ratios (INRs) of virtual interferences are selected in an *ad hoc* manner, and how to determine their parameters needs further investigation.

In the past few years, the convex optimization theory [14] has been successfully exploited in pattern synthesis [15]–[17]. For example, authors of [18] have shown how convex optimization can be utilized to design the optimal pattern for arbitrary antenna arrays. Semidefinite programming (SDP) is employed in [19] and [20] to design nonuniform arrays with desired magnitude responses. Although most of the pattern synthesis problems have non-convex constraints, the convex programming is also useful. By iteratively linearizing the non-convex power pattern constraints, a series of convex subproblems are obtained in [21] and further solved using second-order cone programming (SOCP). Authors of [22] make the non-convex lower bound constraints on the beam pattern convexified, by exploiting the symmetric geometries of linear/planar arrays and adopting a conjugate symmetric weight vector. In [23], the semidefinite relaxation (SDR) technique [24] is employed to approximate the non-convex constraints in the pattern synthesis problem as convex. Apart from the aforementioned methods, there also exist a few approaches attempting to synthesize patterns by utilizing the least-squares method [25], employing the Fast Fourier Transformation (FFT) [26] or excitation matching approach [27].

More recently, we devised several flexible pattern synthesis approaches with array response control scheme. Starting from an arbitrarily-specified weight vector, the accurate array response control ( $A^2$ RC) algorithm [28] synthesizes a desirable beam pattern by iteratively controlling the response of a single angle. However, as reported in [29], the parameter determination of  $A^2$ RC is imperfect and the resulting beam patterns may be distorted. To overcome the drawback of  $A^2$ RC, the weight vector orthogonal decomposition (WORD) algorithm is proposed in [29]. The WORD based pattern synthesis approach shares the same idea as that of  $A^2$ RC. Nevertheless, different from  $A^2$ RC, the weight in WORD is orthogonally decomposed as two parts. By selecting the combining coefficient of the resulting two orthogonal vectors in WORD, the response level at a single direction can be precisely adjusted, and a satisfactory pattern can be synthesized. In WORD algorithm, there are two real-valued candidates for the combining coefficient, and the one that leads to a less pattern variation is selected. In fact, as shall be presented later, one can realize the given response control task by adopting a complex-valued combining coefficient in WORD scheme. Since the candidate set of

The author is with the College of Computer Science and Cyber Security, Chengdu University of Technology, Chengdu 610059, China (e-mail: watersn@126.com).

combining coefficients is incomplete in the existing WORD algorithm, it may lead to performance loss on the ultimate beampattern.

The drawbacks of WORD motivate us to consider a complex-coefficient weight vector orthogonal decomposition (C<sup>2</sup>-WORD) algorithm in this paper, where the combining coefficient is allowed to be complex-valued but not limited to be real-valued. Since the candidate set of weighting coefficients is extended, we can obtain a better performance than WORD in [29]. Moreover, we optimize the parameter of C<sup>2</sup>-WORD by maximizing the white noise gain (WNG) [30]–[32] and obtain a closed-form solution of the ultimate coefficient and weight vector. In addition, we present a detailed analysis on the connection between the proposed C<sup>2</sup>-WORD and the existing A<sup>2</sup>RC. It is shown that C<sup>2</sup>-WORD may degrade into A<sup>2</sup>RC, but outperforms it under general circumstances. By applying C<sup>2</sup>-WORD iteratively, a flexible and effective array pattern synthesis approach is developed and its good performance is validated under various situations. Furthermore, by taking the steering vector uncertainty into consideration, we will utilize C<sup>2</sup>-WORD scheme to realize robust sidelobe control and synthesis, which has not been studied in neither A<sup>2</sup>RC nor WORD.

It should be mentioned that this paper focuses on the main concepts and fundamentals of C<sup>2</sup>-WORD scheme, its application to robust sidelobe control and synthesis will be carried out in the companion paper [33]. This paper is organized as follows. In Section II, the problem formulation of array response control, A<sup>2</sup>RC algorithm and WORD algorithm are briefly introduced. The C<sup>2</sup>-WORD scheme is devised in Section III and its connection with A<sup>2</sup>RC is discussed in Section IV. The application of C<sup>2</sup>-WORD to pattern synthesis is presented in Section V. In Section VI, we present numerical examples to demonstrate the performance of the proposed method. Conclusions are drawn in Section VII.

**Notations:** We use bold upper-case and lower-case letters to represent matrices and vectors, respectively. In particular, we use  $\mathbf{I}$  to denote the identity matrix.  $j \triangleq \sqrt{-1}$ .  $(\cdot)^T$ ,  $(\cdot)^*$  and  $(\cdot)^H$  stand for the transpose, complex conjugate and Hermitian transpose, respectively.  $|\cdot|$  denotes the absolute value and  $\|\cdot\|_2$  denotes the  $l_2$  norm.  $\mathbf{v}(i)$  represents the  $i$ th entry of vector  $\mathbf{v}$ . We use  $\mathbf{B}(i, l)$  to stand for the element at the  $i$ th row and  $l$ th column of matrix  $\mathbf{B}$ .  $\text{Diag}(\cdot)$  represents the diagonal matrix with the components of the input vector as the diagonal elements.  $\Re(\cdot)$  and  $\Im(\cdot)$  denote the real and imaginary parts, respectively.  $\det(\cdot)$  is the determinant of a matrix.  $\propto$  means direct proportion.  $\mathbb{R}$  and  $\mathbb{C}$  denote the sets of all real and all complex numbers, respectively.  $\mathcal{R}(\cdot)$  returns the column space of the input matrix, and  $\mathcal{R}^\perp(\cdot)$  is the orthogonal complementary space of  $\mathcal{R}(\cdot)$ .  $\mathbf{P}_{\mathbf{Z}}$  and  $\mathbf{P}_{\mathbf{Z}}^\perp$  represent the projection matrices onto  $\mathcal{R}(\mathbf{Z})$  and  $\mathcal{R}^\perp(\mathbf{Z})$ , respectively.  $\angle(\cdot)$  returns the argument of a complex number.  $\oplus$  stands for the direct sum operator.

## II. PRELIMINARIES

### A. Response Control Formulation

Without loss of generality and for the sake of clarity, we focus on herein the problem of one-dimensional response

control. The extension to more complicated configurations is straight-forward. First of all, the array power response is expressed as

$$L(\theta, \theta_0) = |\mathbf{w}^H \mathbf{a}(\theta)|^2 / |\mathbf{w}^H \mathbf{a}(\theta_0)|^2 \quad (1)$$

where  $(\cdot)^H$  denotes the conjugate transpose,  $\mathbf{w}$  is the weight vector,  $\theta_0$  is the main beam axis,  $\mathbf{a}(\theta)$  stands for the steering vector in direction  $\theta$ . More exactly, we have

$$\mathbf{a}(\theta) = [g_1(\theta)e^{-j\omega\tau_1(\theta)}, \dots, g_N(\theta)e^{-j\omega\tau_N(\theta)}]^T \quad (2)$$

where  $(\cdot)^T$  denotes the transpose operator,  $j = \sqrt{-1}$  is the imaginary unit,  $\omega$  denotes the operating frequency,  $g_n(\theta)$  denotes the pattern of the  $n$ th element,  $\tau_n(\theta)$  represents the time-delay between the  $n$ th element and the reference point,  $n = 1, \dots, N$ . Notice that the array response in (1) is normalized by the power response at  $\theta_0$  as commonly applied in practice. The problem of array response control can thus be stated as: finding an appropriate weight vector which makes the normalized power response  $L(\theta, \theta_0)$  meet specific requirements.

### B. A<sup>2</sup>RC Algorithm

Recently, an accurate array response control (A<sup>2</sup>RC) algorithm has been developed in [28] to precisely control the response level at one given point. For a given previous weight vector  $\mathbf{w}_{k-1}$  and an angle  $\theta_k$  to be controlled, the weight vector of A<sup>2</sup>RC is updated as

$$\mathbf{w}_k = \mathbf{w}_{k-1} + \mu_k \mathbf{a}(\theta_k) \quad (3)$$

where  $k$  represents the index of step,  $\mu_k$  is the only parameter that can be determined by the desired level  $\rho_k$  at  $\theta_k$ . More specifically, to realize the array response control task at  $\theta_k$ , i.e.,  $L_k(\theta_k, \theta_0) = \rho_k$ , where

$$L_k(\theta, \theta_0) = |\mathbf{w}_k^H \mathbf{a}(\theta)|^2 / |\mathbf{w}_k^H \mathbf{a}(\theta_0)|^2 \quad (4)$$

it has been shown in [28] that  $\mu_k$  locates in a circle:

$$\mathbb{C}_{\mu_k} = \left\{ \mu_k \left| \left\| [\Re(\mu_k), \Im(\mu_k)]^T - \mathbf{c}_{\mu_k} \right\|_2 = R_{\mu_k} \right. \right\} \quad (5)$$

with center  $\mathbf{c}_{\mu} = [-\Re(\mathbf{Q}_k(1, 2)), \Im(\mathbf{Q}_k(1, 2))]^T / \mathbf{Q}_k(2, 2)$  and radius  $R_{\mu} = \sqrt{-\det(\mathbf{Q}_k) / |\mathbf{Q}_k(2, 2)|}$ , where  $\mathbf{Q}_k = [\mathbf{w}_{k-1}, \mathbf{a}(\theta_k)]^H (\mathbf{a}(\theta_k) \mathbf{a}^H(\theta_k) - \rho_k \mathbf{a}(\theta_0) \mathbf{a}^H(\theta_0)) [\mathbf{w}_{k-1}, \mathbf{a}(\theta_k)]$ .

In addition, to generate a less pattern distortion, the optimal  $\mu_{k,*}$  is experimentally selected in [28] as

$$\mu_{k,*} = \mu_{k,s} \triangleq \arg \min_{\mu_k \in \mathbb{C}_{\mu_k}} |\mu_k|. \quad (6)$$

However, a satisfactory performance may not be always guaranteed for A<sup>2</sup>RC, mainly due to its imperfect parameter determination scheme.

### C. WORD Algorithm

To alleviate the drawback of A<sup>2</sup>RC, a novel weight vector orthogonal decomposition (WORD) algorithm was presented in [29] on the foundation of adaptive array theory. More specifically, for a given weight vector  $\mathbf{w}_{k-1}$ , an angle  $\theta_k$  to be

controlled and its desired level  $\rho_k$ , WORD algorithm updates its weight vector as

$$\mathbf{w}_k = [\mathbf{w}_{k-1,\perp} \quad \mathbf{w}_{k-1,\parallel}] \begin{bmatrix} 1 & \beta_k \end{bmatrix}^T, \quad \beta_k \in \mathbb{R} \quad (7)$$

where  $\mathbf{w}_{k-1,\perp}$  and  $\mathbf{w}_{k-1,\parallel}$  are defined as

$$\mathbf{w}_{k-1,\perp} \triangleq \mathbf{P}_{[\mathbf{a}(\theta_k)]}^\perp \mathbf{w}_{k-1}, \quad \mathbf{w}_{k-1,\parallel} \triangleq \mathbf{P}_{[\mathbf{a}(\theta_k)]} \mathbf{w}_{k-1} \quad (8)$$

with  $k$  denoting the step index. In (7), the real-valued  $\beta_k$  can be selected to be either  $\beta_a$  or  $\beta_b$ , both of which can be determined by the desired level  $\rho_k$  at  $\theta_k$ . In [29], it has been derived that

$$\beta_a = \frac{-\Re(\mathbf{B}_k(1,2)) + d}{\mathbf{B}_k(2,2)}, \quad \beta_b = \frac{-\Re(\mathbf{B}_k(1,2)) - d}{\mathbf{B}_k(2,2)} \quad (9)$$

where  $\mathbf{B}_k$  and  $d$  satisfy

$$\mathbf{B}_k = \begin{bmatrix} \mathbf{w}_{\perp}^H \mathbf{a}(\theta_k) \\ \mathbf{w}_{\parallel}^H \mathbf{a}(\theta_k) \end{bmatrix} \begin{bmatrix} \mathbf{w}_{\perp}^H \mathbf{a}(\theta_k) \\ \mathbf{w}_{\parallel}^H \mathbf{a}(\theta_k) \end{bmatrix}^H - \rho_k \begin{bmatrix} \mathbf{w}_{\perp}^H \mathbf{a}(\theta_0) \\ \mathbf{w}_{\parallel}^H \mathbf{a}(\theta_0) \end{bmatrix} \begin{bmatrix} \mathbf{w}_{\perp}^H \mathbf{a}(\theta_0) \\ \mathbf{w}_{\parallel}^H \mathbf{a}(\theta_0) \end{bmatrix}^H \quad (10)$$

$$d = \sqrt{\Re^2(\mathbf{B}_k(1,2)) - \mathbf{B}_k(1,1)\mathbf{B}_k(2,2)}. \quad (11)$$

In (10),  $\mathbf{w}_{\perp}$  and  $\mathbf{w}_{\parallel}$  are the short notations of  $\mathbf{w}_{k-1,\perp}$  and  $\mathbf{w}_{k-1,\parallel}$ , respectively, and will be used in our later discussions. To obtain the ultimate expression of  $\mathbf{w}_k$  that adjusts the response level of  $\theta_k$  to  $\rho_k$ , the one (either  $\beta_a$  or  $\beta_b$ ) that minimizes  $F(\beta) = \|\mathbf{P}_{\mathbf{w}_{k-1}}^\perp \mathbf{w}_k / \|\mathbf{w}_k\|_2\|_2^2$  is selected.

### III. ARRAY RESPONSE CONTROL VIA C<sup>2</sup>-WORD

In this section, we present a new complex-coefficient weight vector orthogonal decomposition (C<sup>2</sup>-WORD) algorithm by modifying the WORD algorithm in [29].

#### A. C<sup>2</sup>-WORD Algorithm

Before presenting the proposed C<sup>2</sup>-WORD algorithm, we first provide the following Lemma.

**Lemma 1:** For  $\forall \beta_k \in \mathbb{R}$  and the corresponding  $\mathbf{w}_k$  in (7), there exists  $\tilde{\beta}_k \in \mathbb{C}$  and a corresponding  $\tilde{\mathbf{w}}_k$  satisfying

$$\tilde{\mathbf{w}}_k = [\mathbf{w}_{\perp} \quad \mathbf{w}_{\parallel}] \begin{bmatrix} 1 & \tilde{\beta}_k \end{bmatrix}^T \quad (12)$$

such that

$$L_k(\theta_k, \theta_0)|_{\mathbf{w}=\tilde{\mathbf{w}}_k} = L_k(\theta_k, \theta_0)|_{\mathbf{w}=\mathbf{w}_k}. \quad (13)$$

Moreover,  $\tilde{\beta}_k$  is non-trivially complex-valued (i.e.,  $\tilde{\beta}_k \notin \mathbb{R}$ ) in most cases.

*Proof:* See Appendix A. ■

Lemma 1 implies that there exists complex-valued  $\tilde{\beta}_k$  leading to the same response level at  $\theta_k$  as that of the prescribed real-valued  $\beta_k$ . Therefore, it is more reasonable to assign a complex-valued  $\beta_k$  in the WORD scheme. This leads to the complex-coefficient weight vector orthogonal decomposition (C<sup>2</sup>-WORD) algorithm as presented next.

More specifically, given the previous weight vector  $\mathbf{w}_{k-1}$ , in order to adjust the array response level of  $\theta_k$  to its desired level  $\rho_k$ , we propose to update the weight vector as

$$\mathbf{w}_k = [\mathbf{w}_{\perp} \quad \mathbf{w}_{\parallel}] \begin{bmatrix} 1 & \beta_k \end{bmatrix}^T, \quad \beta_k \in \mathbb{C}. \quad (14)$$

Different from the weight vector update of WORD in Eqn. (7), the parameter  $\beta_k$  in (14) is complex-valued but not limited

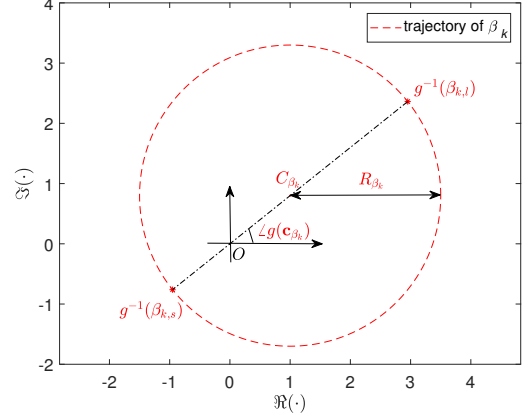


Fig. 1. Geometrical distribution of  $\beta_k$ .

to be real-valued, although we have designated an identical notation (i.e.,  $\beta_k$ ). We will present the benefits later.

To realize the array response control task at  $\theta_k$ , i.e.,

$$L_k(\theta_k, \theta_0) = \rho_k \quad (15)$$

we first find the trajectory of all possible  $\beta_k$ 's in (14). To do so, we substitute (14) into (15) and obtain  $\mathbf{z}_k^H \mathbf{B}_k \mathbf{z}_k = 0$ , where  $\mathbf{z}_k \triangleq [1 \quad \beta_k]^T$ ,  $\mathbf{B}_k$  is a  $2 \times 2$  Hermitian matrix given in (10). After some calculation, we can obtain the following proposition that describes the geometrical distribution of  $\beta_k$ .

**Proposition 1:** Suppose that  $\beta_k$  is a solution of (14) and (15), it can be derived that the trajectory set of  $\beta_k$  is a circle  $\mathbb{C}_{\beta_k}$ :

$$\mathbb{C}_{\beta_k} = \left\{ \beta_k \mid \left\| [\Re(\beta_k), \Im(\beta_k)]^T - \mathbf{c}_{\beta_k} \right\|_2 = R_{\beta_k} \right\} \quad (16)$$

with center

$$\mathbf{c}_{\beta_k} = \frac{1}{\mathbf{B}_k(2,2)} \begin{bmatrix} -\Re(\mathbf{B}_k(1,2)) \\ \Im(\mathbf{B}_k(1,2)) \end{bmatrix} \quad (17)$$

and radius

$$R_{\beta_k} = \sqrt{-\det(\mathbf{B}_k)} / |\mathbf{B}_k(2,2)|. \quad (18)$$

*Proof:* See Appendix B. ■

Fig. 1 presents a geometric interpretation of Proposition 1. It can be readily known that the existing WORD algorithm selects the parameter  $\beta_k$  from the real-valued elements of  $\mathbb{C}_{\beta_k}$ . For our C<sup>2</sup>-WORD algorithm, we have extended the feasible set to complex domain. By doing so, the resulting performance may be improved, since it's possible to select a more appropriate  $\beta_k$  that may not be real-valued.

**Remark 1:** Proposition 1 is valid only if  $\mathbf{B}_k(2,2) \neq 0$ , which is equivalent to  $\rho_k |\mathbf{w}_{\parallel}^H \mathbf{a}(\theta_0)|^2 \neq |\mathbf{w}_{\parallel}^H \mathbf{a}(\theta_k)|^2$  or simply  $\rho_k |\mathbf{a}^H(\theta_k) \mathbf{a}(\theta_0)|^2 \neq |\mathbf{a}^H(\theta_k) \mathbf{a}(\theta_k)|^2$ . As a matter of fact, if  $\rho_k |\mathbf{a}^H(\theta_k) \mathbf{a}(\theta_0)|^2 = |\mathbf{a}^H(\theta_k) \mathbf{a}(\theta_k)|^2$ , one obtains

$$\rho_k = |\mathbf{a}^H(\theta_k) \mathbf{a}(\theta_k)|^2 / |\mathbf{a}^H(\theta_k) \mathbf{a}(\theta_0)|^2 \triangleq \tilde{\rho}_k. \quad (19)$$

Clearly,  $\tilde{\rho}_k$  denotes the array response level at  $\theta_k$  when taking the weight vector as  $\mathbf{a}(\theta_k)$ . Note that the response is normalized by the output at  $\theta_0$ , but its beam axis steers to  $\theta_k \neq \theta_0$ . Therefore, we have  $\tilde{\rho}_k > 1$  under normal

circumstances. For this reason, in the following discussions we reasonably assume that  $\rho_k \in [0, 1]$ , which makes  $\rho_k \neq \tilde{\rho}_k$  or  $\mathbf{B}_k(2, 2) \neq 0$  easily satisfied.

### B. Selection of $\beta_k$

Proposition 1 indicates that there exist infinitely many solutions of (complex-valued)  $\beta_k$  adjusting the array response level of  $\theta_k$  to its desired value  $\rho_k$ . Then, an optimal one, denoted as  $\beta_{k,*}$ , should be selected to further finish the array response control task (15).

In this paper, we optimize the parameter  $\beta_k$  by maximizing the white noise gain (WNG) [30]–[32], which is denoted as  $G$  and satisfies

$$G = \frac{|\mathbf{w}^H \mathbf{a}(\theta_0)|^2}{\|\mathbf{w}\|_2^2}. \quad (20)$$

The WNG measures the signal-to-noise ratio (SNR) improvement, i.e., the ratio of the SNR at the output to the SNR at the input, in the white noise scenario. Combining (14) and Proposition 1, the following constrained problem can be formulated to determine the ultimate  $\beta_{k,*}$ :

$$\max_{\beta_k} G_k = \frac{|\mathbf{w}_k^H \mathbf{a}(\theta_0)|^2}{\|\mathbf{w}_k\|_2^2} \quad (21a)$$

$$\text{subject to } \mathbf{w}_k = [\mathbf{w}_\perp \quad \mathbf{w}_\parallel] \begin{bmatrix} 1 & \beta_k \end{bmatrix}^T \quad (21b)$$

$$\beta_k \in \mathbb{C}_{\beta_k} \quad (21c)$$

where  $\mathbb{C}_{\beta_k}$  is given in (16). Although problem (21) is non-convex, its optimal solution can be analytically expressed as the following proposition described.

**Proposition 2:** The optimal solution  $\beta_{k,*}$  of problem (21) is given by

$$\beta_{k,*} = \beta_{k,l} \triangleq \arg \max_{\beta_k \in \mathbb{C}_{\beta_k}} |\beta_k| = (|\mathbf{c}_{\beta_k}| + R_{\beta_k}) e^{j\angle g(\mathbf{c}_{\beta_k})} \quad (22)$$

where  $g(\cdot)$  is a function satisfying  $g(\mathbf{c}) = \mathbf{c}(1) + j\mathbf{c}(2)$  for a two-dimensional input vector.

*Proof:* See Appendix C. ■

From Proposition 2, we learn that the optimal  $\beta_{k,*}$  has maximum modulo among all  $\beta_k$ 's in  $\mathbb{C}_{\beta_k}$ , refer to  $g^{-1}(\beta_{k,l})$  in Fig. 1 for its location. Once the optimal  $\beta_{k,*}$  is determined, we can express the ultimate weight vector of C<sup>2</sup>-WORD as

$$\mathbf{w}_k = [\mathbf{w}_\perp \quad \mathbf{w}_\parallel] \begin{bmatrix} 1 & \beta_{k,*} \end{bmatrix}^T. \quad (23)$$

In addition, we can derive the following interesting result about the obtained  $\mathbf{w}_k$  in (23).

**Proposition 3:** Taking  $\mathbf{w}_{k-1} = \mathbf{a}(\theta_0)$  and assuming that  $\mathbf{a}^H(\theta_k)\mathbf{a}(\theta_0) \neq 0$ , then the resulting  $\mathbf{w}_k$  in (23) is the global optimal solution of the following problem, i.e.,

$$\max_{\mathbf{w} \in \mathbb{C}^N} \frac{|\mathbf{w}^H \mathbf{a}(\theta_0)|^2}{\|\mathbf{w}\|_2^2} \quad (24a)$$

$$\text{subject to } |\mathbf{w}^H \mathbf{a}(\theta_k)|^2 / |\mathbf{w}^H \mathbf{a}(\theta_0)|^2 = \rho_k. \quad (24b)$$

*Proof:* See Appendix D. ■

According to Proposition 3, the resulting weight vector of C<sup>2</sup>-WORD is optimal in maximizing WNG with the response level constraint (24b), provided that  $\mathbf{a}(\theta_0)$  is taken as the previous weight and  $\mathbf{a}(\theta_k)$  is non-orthogonal to  $\mathbf{a}(\theta_0)$ . It

---

### Algorithm 1 C<sup>2</sup>-WORD Algorithm

---

- 1: prescribe beam axis  $\theta_0$  and index  $k$ , give the previous weight vector  $\mathbf{w}_{k-1}$ , direction  $\theta_k$  and the corresponding desired level  $\rho_k$
  - 2: determine the optimal  $\beta_{k,*}$  in (22)
  - 3: output the new weight vector  $\mathbf{w}_k$  in (23)
- 

should be noted that the constraint of orthogonal decomposition (i.e., (21b)) is not assigned in problem (24). Since  $\beta_{k,*}$  may be complex-valued, the above result may not be true for the traditional WORD algorithm. Finally, we summarize the proposed C<sup>2</sup>-WORD algorithm in Algorithm 1.

### IV. CONNECTION BETWEEN C<sup>2</sup>-WORD AND A<sup>2</sup>RC

In the preceding section, we extend WORD algorithm [29] by allowing the complex-valued coefficient in C<sup>2</sup>-WORD. Since C<sup>2</sup>-WORD optimizes its parameter in a larger range, a more satisfactory performance can be obtained comparing to WORD. To have a better understanding, we next present the connection between C<sup>2</sup>-WORD and the existing A<sup>2</sup>RC in [28]. It is shown that A<sup>2</sup>RC, WORD and C<sup>2</sup>-WORD may obtain identical results under specific circumstances.

To begin with, we re-express the weight vector update of C<sup>2</sup>-WORD, i.e., Eqn. (14), as

$$\begin{aligned} \mathbf{w}_k &= [\mathbf{w}_\perp \quad \mathbf{w}_\parallel] \begin{bmatrix} 1 & \beta_k \end{bmatrix}^T \\ &= \mathbf{P}_{[\mathbf{a}(\theta_k)]}^\perp \mathbf{w}_{k-1} + \beta_k \mathbf{P}_{[\mathbf{a}(\theta_k)]} \mathbf{w}_{k-1} \\ &= \left( \mathbf{I} - \frac{\mathbf{a}(\theta_k) \mathbf{a}^H(\theta_k)}{\mathbf{a}^H(\theta_k) \mathbf{a}(\theta_k)} \right) \mathbf{w}_{k-1} + \frac{\beta_k \mathbf{a}(\theta_k) \mathbf{a}^H(\theta_k)}{\mathbf{a}^H(\theta_k) \mathbf{a}(\theta_k)} \mathbf{w}_{k-1} \\ &= \mathbf{w}_{k-1} + T(\beta_k) \cdot \mathbf{a}(\theta_k) \end{aligned} \quad (25)$$

where the transformation  $T(\beta_k)$  is defined as

$$T(\beta_k) \triangleq \frac{(\beta_k - 1) \mathbf{a}^H(\theta_k) \mathbf{w}_{k-1}}{\mathbf{a}^H(\theta_k) \mathbf{a}(\theta_k)}. \quad (26)$$

Comparing (25) with (3), one can see that the weight vectors of C<sup>2</sup>-WORD and A<sup>2</sup>RC are updated in the same forms, while the difference relies on the parameter selections, see (22) and (6), respectively. In addition, we notice that the component in  $\mathcal{R}^\perp(\mathbf{a}(\theta_k))$  has no contribution to the array response level at  $\theta_k$ , but may affect the responses of the uncontrolled points. From (25), we know that no redundant component has been added into the previous weight  $\mathbf{w}_{k-1}$  for C<sup>2</sup>-WORD algorithm. The resulting benefit may be the less pattern variations at the uncontrolled region.

In fact, the one-one mapping  $T(\cdot)$  can transform  $\beta_k$  of C<sup>2</sup>-WORD into  $\mu_k$  of A<sup>2</sup>RC, and vice versa. Moreover, it's not hard to find that

$$\{T(\beta_k) | L(\theta_k, \theta_0) = \rho_k\} = \{T(\beta_k) | \beta_k \in \mathbb{C}_{\beta_k}\} = \mathbb{C}_{\mu_k}.$$

In addition, C<sup>2</sup>-WORD obtains the same result as A<sup>2</sup>RC under certain circumstances. To see this, we first define

$$\mu_{k,l} \triangleq \arg \max_{\mu_k \in \mathbb{C}_{\mu_k}} |\mu_k|. \quad (27)$$

Then, the following proposition can be established.

**Proposition 4:** For the given  $\mathbf{w}_{k-1}$ ,  $\theta_k$  and  $\rho_k$ , we have  $T(\beta_{k,*}) = \mu_{k,s} = \mu_{k,*}$  if and only if

$$\mathbf{c}_{\beta_k}(2) = 0 \quad \text{and} \quad \mathbf{c}_{\beta_k}(1) \in [0, 1] \quad (28)$$

where  $\mathbf{c}_{\beta_k}$  is given in (17). Meanwhile,  $T(\beta_{k,*}) = \mu_{k,l}$  if and only if

$$\mathbf{c}_{\beta_k}(2) = 0 \quad \text{and} \quad \mathbf{c}_{\beta_k}(1) \in (-\infty, 0) \cup (1, +\infty). \quad (29)$$

Additionally, if  $T(\beta_{k,*}) \in \{\mu_{k,s}, \mu_{k,l}\}$ , we have  $\beta_{k,*} \in \mathbb{R}$ .

*Proof:* See Appendix E. ■

According to Proposition 4, we know that C<sup>2</sup>-WORD results an identical result as A<sup>2</sup>RC, provided that (28) is satisfied. Otherwise, it can be predicted that C<sup>2</sup>-WORD outperforms A<sup>2</sup>RC (in the sense of WNG). Moreover, note that the parameter  $\mu_{k,l}$ , which is defined in (27) and is never selected in A<sup>2</sup>RC, may correspond to the optimal  $\beta_{k,*}$  of C<sup>2</sup>-WORD. In addition, it can be readily find from Proposition 4 that C<sup>2</sup>-WORD may obtain the same result as that of WORD, provided that  $\mathbf{c}_{\beta_k}(2) = 0$ .

Proposition 4 summarizes the condition when C<sup>2</sup>-WORD and A<sup>2</sup>RC becomes equivalent. However, it is still unclear in which concrete cases these two algorithms result an identical weight vector. Before answering this question, we define

$$\bar{\rho}_k \triangleq \frac{|\mathbf{a}^H(\theta_k)\mathbf{a}(\theta_k)|^2}{|\mathbf{a}^H(\theta_0)\mathbf{a}(\theta_0)|^2} = \frac{\|\mathbf{a}(\theta_k)\|_2^4}{\|\mathbf{a}(\theta_0)\|_2^4} \quad (30a)$$

$$\check{\rho}_k \triangleq \frac{|\mathbf{w}_{k-1}^H \mathbf{a}(\theta_k) \mathbf{a}^H(\theta_k) \mathbf{a}(\theta_k)|}{|\mathbf{w}_{k-1}^H \mathbf{a}(\theta_0) \mathbf{a}^H(\theta_0) \mathbf{a}(\theta_k)|}. \quad (30b)$$

Then, the following two corollaries of Proposition 4 can be obtained.

**Corollary 1:** If the previous weight vector is set as  $\mathbf{a}(\theta_0)$ , i.e.,  $\mathbf{w}_{k-1} = \mathbf{a}(\theta_0)$ , then for  $\theta_k \neq \theta_0$  and  $\rho_k$  satisfying

$$0 \leq \rho_k \leq \min\{\bar{\rho}_k, \check{\rho}_k\}, \quad \rho_k \neq \bar{\rho}_k \quad (31)$$

we have  $T(\beta_{k,*}) = \mu_{k,s} = \mu_{k,*}$ . In other words, C<sup>2</sup>-WORD obtains the same weight vector  $\mathbf{w}_k$  as A<sup>2</sup>RC in the above case.

*Proof:* See Appendix F. ■

Corollary 1 shows that C<sup>2</sup>-WORD becomes equivalent to A<sup>2</sup>RC if  $\mathbf{w}_{k-1} = \mathbf{a}(\theta_0)$  taken and the desired level  $\rho_k$  satisfies specific condition, i.e., (31). Note that the Corollary 1 has no limitation on the array configurations. In addition, recalling *Remark 1*, we find that (31) can be easily guaranteed.

In addition, another corollary of Proposition 4, which relates to centro-symmetric arrays [35]–[37], can be established. In brief, a sensor array is called centro-symmetric if its element locations are symmetric with respect to the centroid and the complex characteristics of paired elements are the same. To proceed, we first define the conjugate centro-symmetric vector set  $\mathbb{V}$  as

$$\mathbb{V} \triangleq \left\{ \mathbf{v} \in \mathbb{C}^{N \times 1} \mid \mathbf{v}(i) = \mathbf{v}^*(N - i + 1), \quad \forall i = 1, \dots, N \right\}.$$

It can be readily found that the steering vectors of a centro-symmetric array locate in  $\mathbb{V}$ , provided that the symmetric center is taken as reference. Based on this observation, we can obtain the second corollary of Proposition 4.

---

#### Algorithm 2 C<sup>2</sup>-WORD based Pattern Synthesis Algorithm

---

- 1: give  $\theta_0$ , the desired pattern  $L_d(\theta)$ , the initial weight vector  $\mathbf{w}_0$  and its corresponding pattern  $L_0(\theta, \theta_0)$ , set  $k = 1$
  - 2: **while** 1 **do**
  - 3:   select an angle  $\theta_k$  by comparing  $L_{k-1}(\theta, \theta_0)$  with  $L_d(\theta)$
  - 4:   apply C<sup>2</sup>-WORD to realize  $L_k(\theta_k, \theta_0) = L_d(\theta_k)$ , obtain  $\mathbf{w}_k$  in (23) and the corresponding  $L_k(\theta, \theta_0)$
  - 5:   **if**  $L_k(\theta, \theta_0)$  is not satisfactory **then**
  - 6:     set  $k = k + 1$
  - 7:   **else**
  - 8:     break
  - 9:   **end if**
  - 10: **end while**
  - 11: output  $\mathbf{w}_k$  and  $L_k(\theta, \theta_0)$
- 

**Corollary 2:** For a centro-symmetric array and the prescribed  $\theta_k$  and  $\rho_k$ , if  $\mathbf{w}_0 \in \mathbb{V}$  and

$$0 \leq \rho_k \leq \min\{\bar{\rho}_k, \check{\rho}_k\}, \quad \rho_k \neq \bar{\rho}_k \quad (32)$$

$$\mathbf{w}_\perp^H \mathbf{a}(\theta_0) \mathbf{a}^H(\theta_0) \mathbf{w}_\parallel \geq 0 \quad (33)$$

hold true for  $k = 1, 2, \dots$ . Then C<sup>2</sup>-WORD method will obtain the same weight vector as that of A<sup>2</sup>RC in every step of weight updating. In other words, these two approaches are completely equivalent in this scenario.

*Proof:* See Appendix G. ■

The above Corollary 2 provides a case when A<sup>2</sup>RC becomes equivalent to C<sup>2</sup>-WORD. In this specific scenario, the parameter selection of A<sup>2</sup>RC is optimal in the sense of WNG. For more general cases, the parameter determination of A<sup>2</sup>RC may not be the optimal one. Therefore, the proposed C<sup>2</sup>-WORD algorithm always performs at least as good as A<sup>2</sup>RC.

**Remark 2:** Similar to *Remark 1*, in general we have  $\mathbf{a}^H(\theta_k)\mathbf{a}(\theta_k) > |\mathbf{a}^H(\theta_k)\mathbf{a}(\theta_0)|$ . Based on this observation, the condition  $0 \leq \rho_k < \bar{\rho}_k$  can be guaranteed as long as  $0 \leq \rho_k \leq 1$ . Furthermore, to make  $0 \leq \rho_k \leq \check{\rho}_k$  satisfied, we can simply restrict the desired response level  $\rho_k$  to be lower than its previous level at  $\theta_k$ , i.e.,  $0 \leq \rho_k \leq |\mathbf{w}_{k-1}^H \mathbf{a}(\theta_k)| / |\mathbf{w}_{k-1}^H \mathbf{a}(\theta_0)| = L_{k-1}(\theta_k, \theta_0)$ . Normally,  $L_{k-1}(\theta_k, \theta_0)$  is not greater than 1. Therefore, (32) can be easily satisfied as long as  $0 \leq \rho_k \leq L_{k-1}(\theta_k, \theta_0)$ .

## V. PATTERN SYNTHESIS VIA C<sup>2</sup>-WORD

In this section, the application of C<sup>2</sup>-WORD to pattern synthesis is briefly introduced. Generally speaking, the strategy herein shares a similar concept of pattern synthesis using A<sup>2</sup>RC [28] or WORD [29]. We synthesize a desirable beam-pattern by successively adjusting the response levels at the directions where the specifications do not meet.

More precisely, let  $L_d(\theta)$  be the desired pattern. An initial pattern  $L_0(\theta, \theta_0)$  is firstly obtained by setting the weight vector as  $\mathbf{w}_0$ , and an angle  $\theta_1$ , at which the response level requires adjustment, is selected by comparing the initial pattern with the desired one. Next, the C<sup>2</sup>-WORD scheme is applied to modify the weight vector  $\mathbf{w}_0$  to  $\mathbf{w}_1$ , by setting the desired response level at  $\theta_1$  as  $L_d(\theta_1)$ . Similarly, by comparing

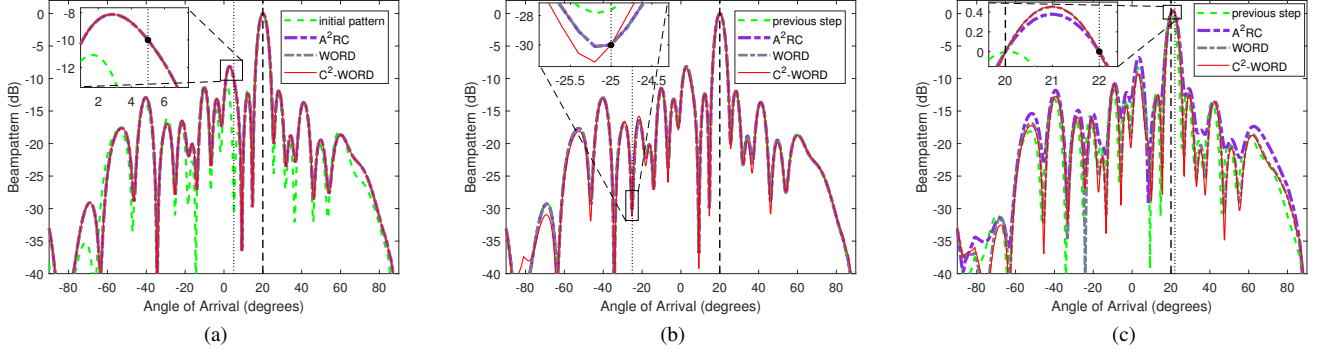


Fig. 2. Illustration of response control for a nonisotropic random array. (a) The synthesized beam patterns at the 1st step. (b) The synthesized beam patterns at the 2nd step. (c) The synthesized beam patterns at the 3rd step.

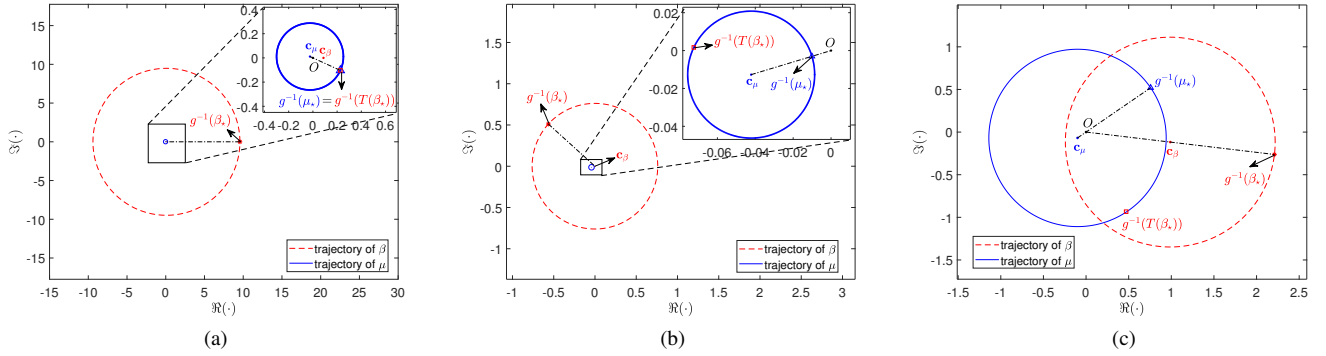


Fig. 3. Geometrical distributions of  $\beta$  and  $\mu$  at different steps. (a) Geometrical distributions of  $\beta$  and  $\mu$  at the 1st step. (b) Geometrical distributions of  $\beta$  and  $\mu$  at the 2nd step. (c) Geometrical distributions of  $\beta$  and  $\mu$  at the 3rd step.

$L_1(\theta, \theta_0)$  with  $L_d(\theta)$ , a second angle  $\theta_2$ , at which the response is needed to be adjusted, is selected. An updated weight vector  $\mathbf{w}_2$  can thus be achieved via C<sup>2</sup>-WORD. The above procedure is carried out successively once a satisfactory array pattern has been obtained. As for how to select the angle to be controlled in every step, we follow the strategy in [28] and [29]. More specifically, for sidelobe synthesis, we select a peak angle where the response difference (from the desired level) is relatively large. For mainlobe synthesis, an angle where the response deviates large from the desired one is chosen. Finally, we summarize the C<sup>2</sup>-WORD based pattern synthesis algorithm in Algorithm 2.

## VI. NUMERICAL RESULTS

In this section, simulations are presented to demonstrate C<sup>2</sup>-WORD on array response control and array pattern synthesis. For comparison purpose, the A<sup>2</sup>RC algorithm in [28], WORD algorithm in [29], convex programming (CP) method in [18] and the semidefinite relaxation (SDR) method in [23] will also be tested if applicable. Unless otherwise specified, we take  $\mathbf{a}(\theta_0)$  as the initial weight for A<sup>2</sup>RC, WORD and the proposed C<sup>2</sup>-WORD.

### A. Response Control of a Nonisotropic Linear Random Array

In this example, we illustrate the performance of C<sup>2</sup>-WORD on array response control and show its advantage over A<sup>2</sup>RC and WORD. More specifically, a 21-element nonisotropic

TABLE I  
PARAMETERS OF THE NONISOTROPIC RANDOM ARRAY

$n$	$x_n(\lambda)$	$l_n(\lambda)$	$\zeta_n(\text{deg})$	$n$	$x_n(\lambda)$	$l_n(\lambda)$	$\zeta_n(\text{deg})$
1	0.00	0.30	0.0	12	5.50	0.20	5.0
2	0.45	0.25	-4.0	13	6.01	0.29	4.0
3	0.95	0.24	5.0	14	6.53	0.20	5.0
4	1.50	0.20	-32	15	7.07	0.26	-9.0
5	2.04	0.26	-3.2	16	7.52	0.21	7.0
6	2.64	0.27	10	17	8.00	0.25	10
7	3.09	0.23	1.0	18	8.47	0.21	6.0
8	3.55	0.24	-10	19	8.98	0.20	-8.0
9	4.05	0.25	0.0	20	9.53	0.26	0.0
10	4.55	0.21	7.0	21	10.01	0.25	5.0
11	5.06	0.20	5.0				

linear random array (see e.g., [5], [11], [28]) is considered. The pattern of the  $n$ th element is given by

$$g_n(\theta) = [\cos(\pi l_n \sin(\theta + \zeta_n)) - \cos(\pi l_n)] / \cos(\theta + \zeta_n) \quad (34)$$

where  $\zeta_n$  and  $l_n$  represent the orientation and length of the element, respectively. More details of the array can be found in Table I, where the element positions (in wavelength) are also specified. To illustrate the effectiveness of the proposed method, we set the beam axis as  $\theta_0 = 20^\circ$  and pre-assign the corresponding desired levels, see Table II for details. The resulting WNGs of A<sup>2</sup>RC, WORD and C<sup>2</sup>-WORD are denoted by  $G_{k,\triangleright}$ ,  $G_{k,\times}$  and  $G_{k,\star}$ , respectively.



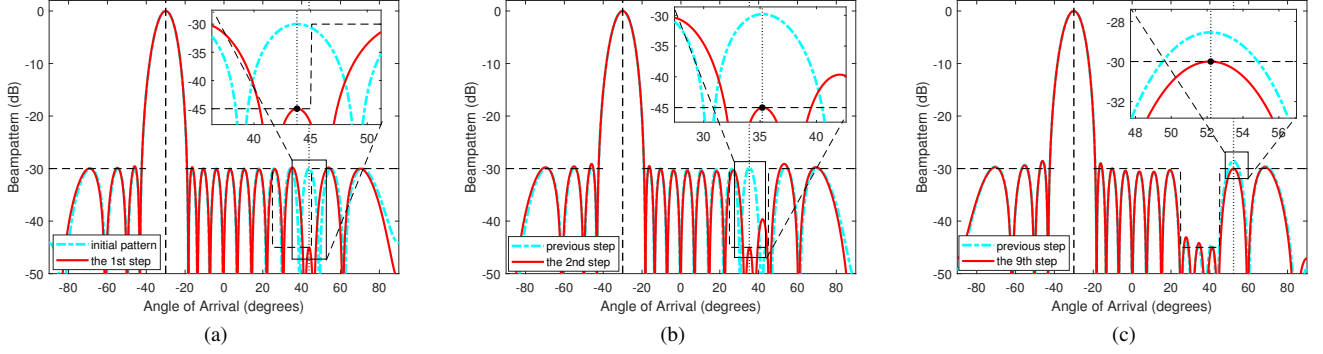


Fig. 4. Synthesis procedure of nonuniform-sidelobe pattern using a ULA (starting from Chebyshev weight). (a) Synthesized pattern at the first step. (b) Synthesized pattern at the second step. (c) Synthesized pattern at the 9th step.

TABLE II  
EXPERIMENT SETTINGS OF RESPONSE CONTROL AND OBTAINED  
PARAMETERS AND WNGS OF DIFFERENT METHODS

	$k = 1$	$k = 2$	$k = 3$
$\theta_k$	$5^\circ$	$-25^\circ$	$22^\circ$
$\rho_k$	$-10$ dB	$-30$ dB	$0$ dB
$\mu_{k,*}$	$0.2270-j0.1034$	$-0.0101-j0.0030$	$0.7577+j0.5199$
$G_{k,*}$	<b>12.9284</b> dB	12.9336 dB	12.1491 dB
$\beta_{k,\times}$	9.5716	0.7606	2.2132
$G_{k,\times}$	<b>12.9284</b> dB	12.9336 dB	12.6085 dB
$T(\beta_{k,\times})$	$0.2270-j0.1034$	$-0.0101-j0.0030$	$0.6499-j0.7894$
$\beta_{k,*}$	9.5716	$-0.5649+j0.5114$	$2.2097-j0.2627$
$G_{k,*}$	<b>12.9284</b> dB	<b>12.9488</b> dB	<b>12.6184</b> dB
$T(\beta_{k,*})$	$0.2270-j0.1034$	$-0.0725+j0.0016$	$0.4703-j0.9336$

Fig. 2 depicts the obtained patterns at different steps. Accordingly, Fig. 3 presents the trajectories of  $\beta$  and  $\mu$ . It can be observed from Fig. 2 that the responses can be adjusted as expected by the three approaches. Table II summarizes the resulting parameters and WNGs. One can see that the resulting WNG of C<sup>2</sup>-WORD algorithm is not less than those of A<sup>2</sup>RC and WORD for each response control step. It is interesting to point out that  $T(\beta_{1,*}) = T(\beta_{1,\times}) = \mu_{1,*}$ , which indicates that the three approaches obtain the same weight vectors in the first step of response control. An intuitive explanation of this result is presented in Fig. 3(a), where we can see that the resulting  $\beta_{1,*}$  is real and  $T(\beta_{1,*})$  coincides exactly with  $\mu_{1,*}$ . This result is actually coincident with the conclusion of Corollary 1. In the 2nd and 3rd steps, C<sup>2</sup>-WORD obtains different beampatterns from those of A<sup>2</sup>RC and WORD, see Fig. 2(b) and Fig. 2(c) for details. The corresponding distributions of  $\beta$  and  $\mu$  are depicted in Fig. 3(b) and Fig. 3(c), from which we find that the resulting  $\beta_{k,*}$ 's are complex-valued and  $T(\beta_{k,*})$  are not coincident with  $\mu_{k,*}$ ,  $k = 2, 3$ .

### B. Pattern Synthesis Using C<sup>2</sup>-WORD

In this section, representative simulations are presented to illustrate the application of C<sup>2</sup>-WORD to pattern synthesis.

1) *Nonuniform Sidelobe Synthesis for a ULA*: In the first example, a 16-element uniformly spaced linear array (ULA) is considered. We steer the beam axis to  $\theta_0 = -30^\circ$ . The desired beampattern has nonuniform sidelobe levels. More specifically,

the upper level is  $-45$  dB in the region  $[25^\circ, 45^\circ]$  and  $-30$  dB in the rest of the sidelobe region. To lower the complexity, we take the initial weight of C<sup>2</sup>-WORD as the Chebyshev weight with a  $-30$  dB sidelobe attenuation. Note that the initial weight is a conjugate centro-symmetric vector, i.e.,  $\mathbf{w}_0 \in \mathbb{V}$ .

Fig. 4 presents several intermediate results when synthesizing pattern by C<sup>2</sup>-WORD. At each response control step, we select one sidelobe peak and then adjust the response to its desired level. From Fig. 4, one can see that the resulting response envelope is similar to the desired one after conducting 9 response control steps. To explore the convergence of the proposed approach, we define  $D_k$  as the maximum response deviation within the set of the sidelobe peak angles at the  $k$ th step (denoted as  $\Omega_s^k$ ), i.e.,

$$D_k \triangleq \max_{\theta \in \Omega_s^k} (L_k(\theta, \theta_0) - L_d(\theta)). \quad (35)$$

The curve of  $D_k$  versus the iterative number  $k$  is depicted in Fig. 5, which clearly shows that  $D_k$  decreases with the increase of iteration. After carrying out 40 response control steps, the resulting  $D_k$  equals approximately to zero and we terminate the synthesis process.

The ultimate pattern of the proposed approach is presented in Fig. 6, where the results of CP, A<sup>2</sup>RC and WORD are also displayed. For both A<sup>2</sup>RC and WORD, we carry out the same iteration steps as that of C<sup>2</sup>-WORD, and the resulting beampatterns of these three approaches are identical in this case. This result is consistent with the prediction of Corollary 2. In addition, we can see that the resulting mainlobe width of CP method is wider, although a qualified sidelobe level is obtained.

To further examine the performance of the proposed approach. We take the mutual coupling into consideration with other settings unchanged. The channel isolation [38] between different elements is  $-20$  dB. The resulting beampatterns of different approaches are presented in Fig. 7. In this case, the proposed C<sup>2</sup>-WORD algorithm obtains a different pattern from those of A<sup>2</sup>RC and WORD. The resulting WNG of our algorithm is 11.30 dB, which is higher than the corresponding 11.01 dB of A<sup>2</sup>RC and WORD. In addition, the resulting WNG of CP method is 10.78 dB and the synthesized beampattern is not aligned with the desired one.

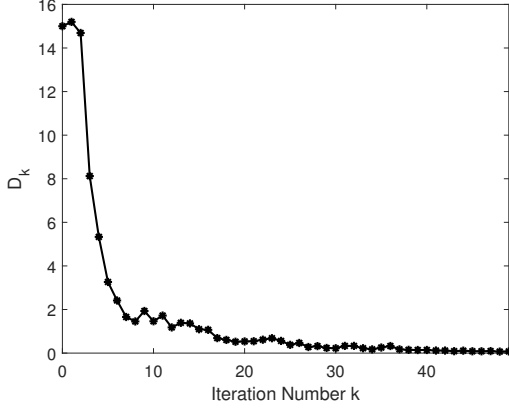


Fig. 5. Maximum response deviation  $D_k$  versus the iteration number.

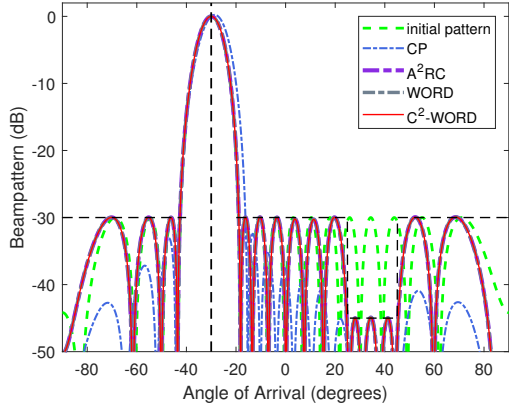


Fig. 6. Comparison of the synthesized patterns.

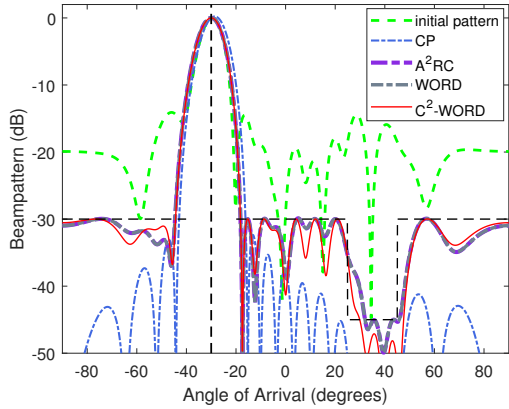


Fig. 7. Synthesized patterns with non-uniform sidelobe for a ULA with mutual coupling.

## 2) Synthesizing Flat-Top Pattern for Linear Random Array:

In this example, we consider a linear random array, with its element location specifying in Table III. In this case, the desired pattern has both sidelobe and mainlobe constraints. More specifically, the upper level is  $-35\text{dB}$  in the region  $[60^\circ, 75^\circ]$  and  $-25\text{dB}$  in the rest of the sidelobe region. For mainlobe response, its desired level is  $0\text{dB}$  in the pre-assigned

TABLE III  
ELEMENT LOCATIONS OF LINEAR RANDOM ARRAY AND WEIGHTS  
OBTAINED BY THE PROPOSED METHOD

$n$	$x_n(\lambda)$	$w_n$	$n$	$x_n(\lambda)$	$w_n$
1	0.00	$0.2523e^{+j0.0468}$	9	3.99	$0.8648e^{-j2.8313}$
2	0.47	$0.0239e^{+j0.6417}$	10	4.48	$0.0802e^{+j1.0755}$
3	1.01	$0.1932e^{-j2.3044}$	11	4.96	$0.9415e^{+j0.2068}$
4	1.47	$0.3330e^{+j3.0465}$	12	5.43	$1.0000e^{+j0.0084}$
5	1.97	$0.2863e^{+j0.3971}$	13	5.94	$0.7295e^{+j0.0597}$
6	2.54	$0.6463e^{+j0.2904}$	14	6.49	$0.7338e^{+j0.0040}$
7	3.06	$0.1202e^{+j0.0574}$	15	6.98	$0.6187e^{+j0.1650}$
8	3.53	$0.7930e^{-j2.8431}$	16	7.46	$0.3340e^{-j0.2297}$

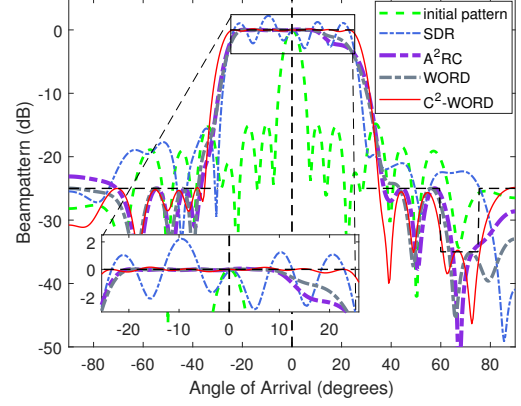


Fig. 8. Synthesized patterns with flat-top mainlobe and broad-notch sidelobe for a random linear array with mutual coupling.

region  $[-25^\circ, 25^\circ]$ . In addition, we consider mutual coupling with a  $-25\text{dB}$  channel isolation between different elements. After carrying out 300 response control steps, the proposed  $C^2$ -WORD approach synthesizes a desirable beam pattern and the resulting weightings are listed in Table III.

Fig. 8 presents the resulting patterns of  $C^2$ -WORD,  $A^2$ RC, WORD (all with the same iteration steps) and SDR. We can see that the  $C^2$ -WORD approach obtains satisfactory responses at both sidelobe and mainlobe region. The ripple of the mainlobe response is about  $0.3\text{dB}$ , which is less than those of the other three methods. Note that both  $A^2$ RC and WORD lead to some pattern distortions at the mainlobe region. For the SDR approach, the resulting mainlobe ripple is large and the synthesized sidelobe is not qualified. The reason probably is that the ultimate weight of SDR method may not satisfy the pre-defined constraints, due to the relaxation operator to the original problem.

3) *Pattern Synthesis for Conformal Array:* To further show the effectiveness of the proposed  $C^2$ -WORD algorithm, we follow the array configuration in [39] and consider a circular arc array that conforms to a cylindrical surface as shown in Fig. 9. The element number is 16 and the distance between adjacent elements is half a wavelength. The  $\theta_c$  in Fig. 9 is set as  $60^\circ$ . In addition, we take the element polarized pattern and mutual coupling effect into consideration. More specifically, the element pattern follows the lowest order circular patch model [40]–[42], and the beam pattern can be analytically expressed as described in [43]. As for mutual coupling, the



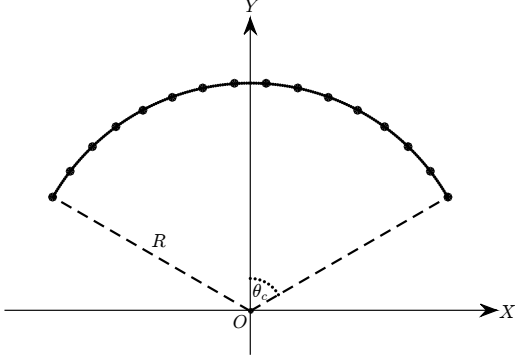


Fig. 9. Illustration of a circular arc array.

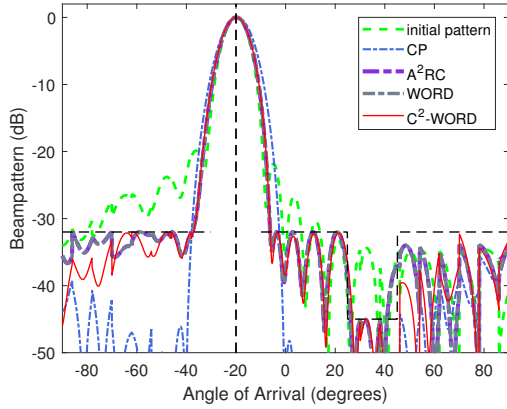


Fig. 10. Synthesized patterns for a circular arc array.

corresponding channel isolation between different elements is  $-25\text{dB}$ . In this case, we steer the beam axis to  $\theta_0 = -20^\circ$ . The desired pattern has  $-45\text{dB}$  upper level in the region  $[25^\circ, 45^\circ]$  and is expected to be lower than  $-32\text{dB}$  in the rest of the sidelobe region. For simplicity, we only consider the pattern that is coplanar to the array plane, although the extensions are straightforward. Fig. 10 depicts the resulting patterns of different approaches. One can see that our approach synthesizes a more satisfactory pattern than those of CP,  $A^2\text{RC}$  and WORD.

## VII. CONCLUSIONS

In this paper, we have presented a new scheme named complex-coefficient weight vector orthogonal decomposition ( $C^2\text{-WORD}$ ). The  $C^2\text{-WORD}$  algorithm is modified from the existing WORD method. We have extended the WORD algorithm by allowing a complex-valued combining coefficient in the devised  $C^2\text{-WORD}$  algorithm. Moreover, parameter selection has been carried out to maximize the white noise gain (WNG), and a closed-form solution of weight vector updating has been obtained. In addition, we have presented the benefits of  $C^2\text{-WORD}$  (comparing to WORD), and have discussed the connection between  $C^2\text{-WORD}$  and the existing  $A^2\text{RC}$  algorithm. It has been shown that  $C^2\text{-WORD}$  may degrade into  $A^2\text{RC}$  under specific circumstances, and always performs at least as good as  $A^2\text{RC}$  and WORD in the sense of WNG.

The application of  $C^2\text{-WORD}$  to array pattern synthesis has been studied and validated with various examples. Based on the fundamentals developed in this paper, a further application of  $C^2\text{-WORD}$  to robust sidelobe control and synthesis will be considered in [33], by taking the array steering vector uncertainties into consideration.

## APPENDIX A PROOF OF LEMMA 1

For simplicity, we omit the subscript  $k$  of  $\beta$  and  $\tilde{\beta}$  in sequel. To proof Lemma 1, we can find a specific  $\tilde{\beta} \in \mathbb{C}$  and the corresponding  $\tilde{\mathbf{w}}_k$  in (12) making (13) satisfied. To this end, for any given  $\beta \in \mathbb{R}$ , we set  $\tilde{\beta}$  as

$$\tilde{\beta} = \beta + j\zeta \quad (36)$$

where  $\zeta$  is defined as

$$\zeta \triangleq 2\beta^2\eta_i / (|\xi_\perp|^2 + 2\beta\eta_r) \in \mathbb{R} \quad (37)$$

with  $\eta_r = \Re(\xi_\parallel \xi_\perp^*)$ ,  $\eta_i = \Im(\xi_\parallel \xi_\perp^*)$ ,  $\xi_\parallel = \mathbf{w}_\parallel^H \mathbf{a}(\theta_0)$ ,  $\xi_\perp = \mathbf{w}_\perp^H \mathbf{a}(\theta_0)$ . Since both  $\beta$  and  $\zeta$  are real-valued, we have

$$\Re((\beta - j\zeta)\xi_\parallel \xi_\perp^*) = \beta\eta_r + \zeta\eta_i. \quad (38)$$

On the other hand, one can readily obtain from (37) that  $2\beta^2\eta_i = \zeta(|\xi_\perp|^2 + 2\beta\eta_r)$ . On this basis, it can be easily derived that  $2\beta^2\zeta\eta_i + 2\beta^3\eta_r = \zeta^2(|\xi_\perp|^2 + 2\beta\eta_r) + 2\beta^3\eta_r$ , which can be equivalently re-expressed as

$$2\beta^2(\beta\eta_r + \zeta\eta_i) = \zeta^2|\xi_\perp|^2 + 2(\beta^2 + \zeta^2)\beta\eta_r. \quad (39)$$

Combining (38) and (39), one can obtain that

$$\begin{aligned} & \underbrace{\beta^2 (|\xi_\perp|^2 + (\beta^2 + \zeta^2)|\xi_\parallel|^2 + 2\Re((\beta - j\zeta)\xi_\parallel \xi_\perp^*))}_{|\xi_\perp + (\beta - j\zeta)\xi_\parallel|^2} \\ &= (\beta^2 + \zeta^2) \underbrace{(|\xi_\perp|^2 + \beta^2|\xi_\parallel|^2 + 2\beta\eta_r)}_{|\xi_\perp + \beta\xi_\parallel|^2} \end{aligned} \quad (40)$$

and then

$$\frac{(\beta^2 + \zeta^2)}{|\xi_\perp + (\beta - j\zeta)\xi_\parallel|^2} = \frac{\beta^2}{|\xi_\perp + \beta\xi_\parallel|^2}. \quad (41)$$

Substituting  $\tilde{\mathbf{w}}_k = \mathbf{w}_\perp + \tilde{\beta}\mathbf{w}_\parallel$  into  $L_k(\theta_k, \theta_0)$  and combining (41), we have

$$\begin{aligned} L_k(\theta_k, \theta_0)|_{\mathbf{w}=\tilde{\mathbf{w}}_k} &= \frac{(\beta^2 + \zeta^2)|\mathbf{w}_\parallel^H \mathbf{a}(\theta_k)|^2}{|\xi_\perp + (\beta - j\zeta)\xi_\parallel|^2} \\ &= \frac{\beta^2|\mathbf{w}_\parallel^H \mathbf{a}(\theta_k)|^2}{|\xi_\perp + \beta\xi_\parallel|^2} \\ &= L_k(\theta_k, \theta_0)|_{\mathbf{w}=\mathbf{w}_k} \end{aligned} \quad (42)$$

which indicates that (13) holds true. Moreover, we know from (36) that  $\tilde{\beta} \notin \mathbb{R}$  if only  $\beta \neq 0$  and  $\eta_i \neq 0$ . This completes the proof of Lemma 1.

## APPENDIX B PROOF OF PROPOSITION 1

For the sake of clarity, we may omit the subscript  $k$  in sequel. To solve  $\mathbf{z}^H \mathbf{B} \mathbf{z} = 0$ , we take eigenvalue decomposition of  $\mathbf{B}$ , i.e.,  $\mathbf{B} = \mathbf{U} \mathbf{\Lambda} \mathbf{U}^H$ , where  $\mathbf{U}$  is a unitary matrix,  $\mathbf{\Lambda} = \text{Diag}([\lambda_1, \lambda_2])$  with  $\lambda_1$  and  $\lambda_2$  denoting eigenvalues of  $\mathbf{B}$ . Define  $\mathbf{y} \triangleq \mathbf{U}^H \mathbf{z}$ . Then  $\mathbf{z}^H \mathbf{B} \mathbf{z} = 0$  can be equivalently expressed as  $\mathbf{y}^H \mathbf{\Lambda} \mathbf{y} = 0$ , and further

$$\lambda_1 |\mathbf{y}(1)|^2 + \lambda_2 |\mathbf{y}(2)|^2 = 0. \quad (43)$$

Since  $\lambda_1 \lambda_2 = \det(\mathbf{B}) = -\rho_k |\mathbf{w}_\perp^H \mathbf{a}(\theta_0)|^2 |\mathbf{w}_\parallel^H \mathbf{a}(\theta_k)|^2 \leq 0$ , we learn that (43) can be solved. Let us first denote that

$$\mathbf{U} = \begin{bmatrix} u_{11} & u_{12} \\ u_{21} & u_{22} \end{bmatrix}. \quad (44)$$

Since  $\mathbf{y} = \mathbf{U}^H \mathbf{z}$ , we have  $\mathbf{y}(1) = u_{11}^* + u_{21}^* \beta$  and  $\mathbf{y}(2) = u_{12}^* + u_{22}^* \beta$ . Then, one can obtain that

$$\begin{aligned} & \lambda_1 |\mathbf{y}(1)|^2 + \lambda_2 |\mathbf{y}(2)|^2 \\ &= \lambda_1 |u_{11}^* + u_{21}^* \beta|^2 + \lambda_2 |u_{12}^* + u_{22}^* \beta|^2 \\ &= \underbrace{\lambda_1 |u_{11}|^2 + \lambda_2 |u_{12}|^2}_{\mathbf{B}(1,1)} + \underbrace{(\lambda_1 u_{21}^* u_{11} + \lambda_2 u_{22}^* u_{12}) \beta}_{\mathbf{B}(1,2)} + \\ & \quad \underbrace{(\lambda_1 u_{11}^* u_{21} + \lambda_2 u_{12}^* u_{22}) \beta^*}_{\mathbf{B}(2,1)} + \underbrace{(\lambda_1 |u_{21}|^2 + \lambda_2 |u_{22}|^2) |\beta|^2}_{\mathbf{B}(2,2)} \\ &= \mathbf{B}(1,1) + 2\Re(\mathbf{B}(1,2) \cdot \beta) + \mathbf{B}(2,2) |\beta|^2 \\ &= \mathbf{B}(1,1) + 2\Re(\mathbf{B}(1,2)) \cdot \Re(\beta) - 2\Im(\mathbf{B}(1,2)) \cdot \Im(\beta) \\ & \quad + \mathbf{B}(2,2) (\Re^2(\beta) + \Im^2(\beta)) \\ &= 0 \end{aligned} \quad (45)$$

where we have utilized the identities that

$$\mathbf{B}(1,1) = \lambda_1 |u_{11}|^2 + \lambda_2 |u_{12}|^2 \quad (46a)$$

$$\mathbf{B}(1,2) = \lambda_1 u_{21}^* u_{11} + \lambda_2 u_{22}^* u_{12} \quad (46b)$$

$$\mathbf{B}(2,1) = \lambda_1 u_{11}^* u_{21} + \lambda_2 u_{12}^* u_{22} \quad (46c)$$

$$\mathbf{B}(2,2) = \lambda_1 |u_{21}|^2 + \lambda_2 |u_{22}|^2. \quad (46d)$$

Eqn. (45) can be rewritten as

$$\begin{aligned} & \left( \Re(\beta) + \frac{\Re(\mathbf{B}(1,2))}{\mathbf{B}(2,2)} \right)^2 + \left( \Im(\beta) - \frac{\Im(\mathbf{B}(1,2))}{\mathbf{B}(2,2)} \right)^2 \\ &= -\frac{\mathbf{B}(1,1)}{\mathbf{B}(2,2)} + \frac{|\mathbf{B}(1,2)|^2}{\mathbf{B}^2(2,2)} = -\frac{\det(\mathbf{B})}{\mathbf{B}^2(2,2)} \end{aligned} \quad (47)$$

which implies that  $[\Re(\beta) \ \Im(\beta)]^T$  locates in a circle with center  $\mathbf{c}_\beta = [-\Re(\mathbf{B}(1,2)) \ \Im(\mathbf{B}(1,2))]^T / \mathbf{B}(2,2)$  and radius  $R_\beta = \sqrt{-\det(\mathbf{B}) / |\mathbf{B}(2,2)|}$ . This completes the proof.

## APPENDIX C PROOF OF PROPOSITION 2

Substituting (21b) into (21a) and recalling the constraint (15), we have

$$G_k \propto J(\beta_k) \triangleq \frac{|\beta_k|^2 |\mathbf{w}_\parallel^H \mathbf{a}(\theta_k)|^2}{\|\mathbf{w}_\perp\|_2^2 + |\beta_k|^2 \|\mathbf{w}_\parallel\|_2^2}. \quad (48)$$

Moreover, it is not hard to derive that

$$\frac{\partial J(\beta_k)}{\partial |\beta_k|^2} = \frac{|\mathbf{w}_\parallel^H \mathbf{a}(\theta_k)|^2 \|\mathbf{w}_\perp\|_2^2}{(\|\mathbf{w}_\perp\|_2^2 + |\beta_k|^2 \|\mathbf{w}_\parallel\|_2^2)^2} \geq 0 \quad (49)$$

which implies that the optimization function  $J(\beta_k)$  is monotonically non-decreasing with the increase of  $|\beta_k|$ . According to this observation, one can readily obtain that

$$\beta_{k,*} = \arg \max_{\beta_k \in \mathbb{C}_{\beta_k}} |\beta_k|. \quad (50)$$

Recalling Proposition 1 and Fig. 1, we know that the  $\beta_k$  with maximum modulo among  $\mathbb{C}_{\beta_k}$  is the intersection point of circle  $\mathbb{C}_{\beta_k}$  with the line that passes  $O$  and  $\mathbf{c}_{\beta_k}$ , see  $g^{-1}(\beta_{k,l})$  in Fig. 1. Mathematically, it can be readily obtained that

$$\beta_{k,*} = (|\mathbf{c}_{\beta_k}| + R_{\beta_k}) e^{j \angle g(\mathbf{c}_{\beta_k})}. \quad (51)$$

This completes the proof.

## APPENDIX D PROOF OF PROPOSITION 3

We divide the proof details of Proposition 3 into the following 3 steps.

*Step 1:* In the first step, we will show that the optimal solution (denoted as  $\mathbf{w}_\triangleright$ ) of problem (24) satisfies

$$\mathbf{w}_\triangleright \in \mathcal{R}([\mathbf{a}(\theta_0), \mathbf{a}(\theta_k)]). \quad (52)$$

To this end, it should be noted that the space  $\mathbb{C}^N$  satisfies

$$\mathbb{C}^N = \mathcal{R}([\mathbf{a}(\theta_0), \mathbf{a}(\theta_k)]) \oplus \mathcal{R}^\perp([\mathbf{a}(\theta_0), \mathbf{a}(\theta_k)]). \quad (53)$$

In other words, we can split  $\forall \mathbf{w} \in \mathbb{C}^N$  as

$$\mathbf{w} = \mathbf{s}_1 + \mathbf{s}_2 \quad (54)$$

where  $\mathbf{s}_1 \in \mathcal{R}([\mathbf{a}(\theta_0), \mathbf{a}(\theta_k)])$ ,  $\mathbf{s}_2 \in \mathcal{R}^\perp([\mathbf{a}(\theta_0), \mathbf{a}(\theta_k)])$  and  $\mathbf{s}_1^H \mathbf{s}_2 = 0$ . Notice that

$$\mathbf{w}^H \mathbf{a}(\theta_k) = \mathbf{s}_1^H \mathbf{a}(\theta_k), \quad \|\mathbf{w}\|_2^2 = \|\mathbf{s}_1\|_2^2 + \|\mathbf{s}_2\|_2^2. \quad (55)$$

Clearly, to maximize the utility function in (24a), one shall set  $\mathbf{s}_2$  as zero. This completes the proof of (52).

*Step 2:* In the second step, we will show that

$$\mathcal{R}([\mathbf{a}(\theta_0), \mathbf{a}(\theta_k)]) = \mathcal{R}([\mathbf{w}_\perp, \mathbf{w}_\parallel]). \quad (56)$$

To see this, we recall the expressions of  $\mathbf{w}_\perp$  and  $\mathbf{w}_\parallel$  in (8) and obtain that

$$[\mathbf{w}_\perp, \mathbf{w}_\parallel] = [\mathbf{a}(\theta_0), \mathbf{a}(\theta_k)] \mathbf{T} \quad (57)$$

where  $\mathbf{T}$  is given by

$$\mathbf{T} = \begin{bmatrix} 1 & 0 \\ -\frac{\mathbf{a}^H(\theta_k) \mathbf{a}(\theta_0)}{\|\mathbf{a}(\theta_k)\|_2^2} & \frac{\mathbf{a}^H(\theta_k) \mathbf{a}(\theta_0)}{\|\mathbf{a}(\theta_k)\|_2^2} \end{bmatrix}. \quad (58)$$

If  $\mathbf{a}^H(\theta_k) \mathbf{a}(\theta_0) \neq 0$ , one can see that  $\mathbf{T}$  is invertible. Thus, Eqn. (57) indicates that  $[\mathbf{w}_\perp, \mathbf{w}_\parallel]$  spans the same column space as that of  $[\mathbf{a}(\theta_0), \mathbf{a}(\theta_k)]$ . This completes the proof of (56).

*Step 3:* In the third step, we will complete the proof of Proposition 3 by showing that

$$\mathbf{w}_\triangleright = c [\mathbf{w}_\perp \ \mathbf{w}_\parallel] \begin{bmatrix} 1 & \beta_{k,*} \end{bmatrix}^T, \quad c \neq 0. \quad (59)$$

Toward this end, we recall (52) and reformulate problem (24) as

$$\max_{c_1, c_2 \in \mathbb{C}} \frac{|\mathbf{w}^H \mathbf{a}(\theta_0)|^2}{\|\mathbf{w}\|_2^2} \quad (60a)$$

$$\text{subject to } |\mathbf{w}^H \mathbf{a}(\theta_k)|^2 / |\mathbf{w}^H \mathbf{a}(\theta_0)|^2 = \rho_k \quad (60b)$$

$$\mathbf{w} = c_1 \mathbf{a}(\theta_0) + c_2 \mathbf{a}(\theta_k). \quad (60c)$$

It should be pointed out that  $c_1 \neq 0$ , otherwise, we can obtain  $\rho_k = |\mathbf{w}_\perp^H \mathbf{a}(\theta_k)|^2 / |\mathbf{w}_\perp^H \mathbf{a}(\theta_0)|^2 = |\mathbf{a}^H(\theta_k) \mathbf{a}(\theta_k)|^2 / |\mathbf{a}^H(\theta_k) \mathbf{a}(\theta_0)|^2 = \tilde{\rho}_k > 1$ , which is in contraction with the setting of  $\rho_k \leq 1$ , see *Remark 1*. According to (57),  $\mathbf{w} = c_1 \mathbf{a}(\theta_0) + c_2 \mathbf{a}(\theta_k)$  can be equivalently expressed as

$$\mathbf{w} = [\mathbf{w}_\perp, \mathbf{w}_\parallel] \mathbf{T}^{-1} [c_1, c_2]^T = c_1 [\mathbf{w}_\perp, \mathbf{w}_\parallel] [1, \gamma]^T \quad (61)$$

where  $\gamma$  is a specific parameter determined by  $c_1, c_2, \mathbf{a}(\theta_0)$  and  $\mathbf{a}(\theta_k)$ . Then, instead of solving problem (60) or the original problem (24), we can formulate the following problem:

$$\max_{\gamma \in \mathbb{C}} \frac{|\mathbf{w}^H \mathbf{a}(\theta_0)|^2}{\|\mathbf{w}\|_2^2} \quad (62a)$$

$$\text{subject to } |\mathbf{w}^H \mathbf{a}(\theta_k)|^2 / |\mathbf{w}^H \mathbf{a}(\theta_0)|^2 = \rho_k \quad (62b)$$

$$\mathbf{w} = [\mathbf{w}_\perp, \mathbf{w}_\parallel] [1, \gamma]^T \quad (62c)$$

which is equivalent to problem (21). Combining the result of Proposition 2, we know that the resulting  $\mathbf{w}_k$  in (23) is the optimal solution of problem (24) under specific prerequisites. This completes the proof of Proposition 3.

#### APPENDIX E PROOF OF PROPOSITION 4

To begin with, we first proof:

$$T(\beta_{k,*}) = \mu_{k,s} \Leftrightarrow \mathbf{c}_{\beta_k}(2) = 0 \text{ and } \mathbf{c}_{\beta_k}(1) \in [0, 1]. \quad (63)$$

Toward this end, we define  $\hat{\beta}_k \triangleq T^{-1}(\mu_{k,s})$ . Then, it's not hard to obtain that

$$\mu_{k,s} = \arg \min_{\mu_k \in \mathbb{C}_{\mu_k}} |\mu_k| \Leftrightarrow \quad (64a)$$

$$T(\hat{\beta}_k) = \arg \min_{T(\beta_k) \in \mathbb{C}_{\mu_k}} |T(\beta_k)| \Leftrightarrow \quad (64b)$$

$$\hat{\beta}_k = \arg \min_{\beta_k \in \mathbb{C}_{\beta_k}} |T(\beta_k)| \Leftrightarrow \quad (64c)$$

$$\hat{\beta}_k = \arg \min_{\beta_k \in \mathbb{C}_{\beta_k}} |\beta_k - 1|. \quad (64d)$$

Recalling Proposition 2,  $\beta_{k,*}$  satisfies

$$\beta_{k,*} = \arg \max_{\beta_k \in \mathbb{C}_{\beta_k}} |\beta_k|. \quad (65)$$

Combining (64) and (65), one learns that  $\mu_{k,s} = T(\beta_{k,*})$  or equivalently  $\hat{\beta}_k = \beta_{k,*}$  if and only if

$$\arg \min_{\beta_k \in \mathbb{C}_{\beta_k}} |\beta_k - 1| = \arg \max_{\beta_k \in \mathbb{C}_{\beta_k}} |\beta_k|. \quad (66)$$

Recalling Proposition 1 and Fig. 1, we know that (66) is true if and only the following two conditions are satisfied.

The first condition is that

$$\mathbf{c}_{\beta_k}(2) = 0. \quad (67)$$

This is because that the optimal value of the right side of (66) locates in the intersection of the circle  $\mathbb{C}_{\beta_k}$  and the line that passes  $\mathbf{c}_{\beta_k}$  and  $\mathbf{O}$ . And the optimal solution of the left side of (66) locates in the intersection of  $\mathbb{C}_{\beta_k}$  and the line that passes  $\mathbf{c}_{\beta_k}$  and the point  $[1, 0]^T$ . To obtain a unique  $\beta_k$  that simultaneously optimizes the both sides of (66), the three points, i.e.,  $\mathbf{O}$ ,  $\mathbf{c}_{\beta_k}$  and  $[1, 0]^T$  must be colinear, i.e.,  $\mathbf{c}_{\beta_k}(2) = 0$ , otherwise, (66) cannot be true.

On the basis of the above condition (i.e., (67)), the second condition that makes (66) satisfied is

$$\mathbf{c}_{\beta_k}(1) \in [0, 1]. \quad (68)$$

One can readily verify that (66) holds true only if both (67) and (68) are true.

On the contrary, it can be similarly validated that (66) is satisfied, provided that (67) and (68) are true. To summarize, we learn that  $T(\beta_{k,*}) = \mu_{k,s} = \mu_{k,*}$  if and only if (67) and (68) are satisfied. The derivation of  $T(\beta_{k,*}) = \mu_{k,l}$  is similar, we omit it for the sake of space limitation.

In addition, if  $\mathbf{c}_{\beta_k}(2) = 0$ ,  $\angle g(\mathbf{c}_{\beta_k})$  would equal to 0 or  $\pi$ . Combining the expression of  $\beta_{k,*}$  in (22), one can readily obtain that  $\beta_{k,*} \in \mathbb{R}$ , provided that  $T(\beta_{k,*}) \in \{\mu_{k,s}, \mu_{k,l}\}$ . This completes the proof of Proposition 4.

#### APPENDIX F PROOF OF COROLLARY 1

We divide the proof derivation into three steps.

*Step 1:* In the first step, we will proof that

$$\mathbf{B}_k(1, 2) \in \mathbb{R} \text{ and } \mathbf{B}_k(1, 2) \leq 0 \quad (69)$$

provided that  $\mathbf{w}_{k-1} = \mathbf{a}(\theta_0)$ . To do so, we substitute  $\mathbf{w}_{k-1}$  into  $\mathbf{B}_k(1, 2)$  and obtain that

$$\begin{aligned} \frac{\mathbf{B}_k(1, 2)}{-\rho_k} &= \mathbf{w}_\perp^H \mathbf{a}(\theta_0) \mathbf{a}^H(\theta_0) \mathbf{w}_\parallel \\ &= (\mathbf{w}_{k-1} - \mathbf{w}_\parallel)^H \mathbf{a}(\theta_0) \mathbf{a}^H(\theta_0) \mathbf{w}_\parallel \\ &= \frac{\|\mathbf{a}(\theta_0)\|_2^2 \cdot |\mathbf{a}^H(\theta_0) \mathbf{a}(\theta_k)|^2}{\|\mathbf{a}(\theta_k)\|_2^2} - \frac{|\mathbf{a}^H(\theta_0) \mathbf{a}(\theta_k)|^4}{\|\mathbf{a}(\theta_k)\|_2^4} \end{aligned} \quad (70)$$

which indicates that  $\mathbf{B}_k(1, 2) \in \mathbb{R}$ . Moreover, from (70), one can see that  $\mathbf{B}_k(1, 2) \leq 0$  is equivalent to

$$\frac{\|\mathbf{a}(\theta_0)\|_2^2 \cdot |\mathbf{a}^H(\theta_0) \mathbf{a}(\theta_k)|^2}{\|\mathbf{a}(\theta_k)\|_2^2} \geq \frac{|\mathbf{a}^H(\theta_0) \mathbf{a}(\theta_k)|^4}{\|\mathbf{a}(\theta_k)\|_2^4} \quad (71)$$

or simply

$$\|\mathbf{a}(\theta_0)\|_2^2 \cdot \|\mathbf{a}(\theta_k)\|_2^2 \geq |\mathbf{a}^H(\theta_0) \mathbf{a}(\theta_k)|^2. \quad (72)$$

Since (72) is a direct result of Cauchy-Schwarz inequality, we know  $\mathbf{B}_k(1, 2) \leq 0$  is true. Thus, the proof of (69) is completed.

*Step 2:* In this step, we will show that if  $\rho_k < \tilde{\rho}_k$ , then

$$\mathbf{B}_k(2, 2) > 0. \quad (73)$$

To do so, we recall the expression of  $\mathbf{B}_k(2, 2)$  and convert (73) as

$$|\mathbf{w}_\parallel^H \mathbf{a}(\theta_k)|^2 > \rho_k |\mathbf{w}_\parallel^H \mathbf{a}(\theta_0)|^2. \quad (74)$$

Since

$$\mathbf{w}_{\parallel} = \frac{\mathbf{a}(\theta_k)\mathbf{a}^H(\theta_k)\mathbf{w}_{k-1}}{\mathbf{a}^H(\theta_k)\mathbf{a}(\theta_k)} \quad (75)$$

one can further rewrite Eqn. (74) as

$$\rho_k < \frac{|\mathbf{w}_{\parallel}^H \mathbf{a}(\theta_k)|^2}{|\mathbf{w}_{\parallel}^H \mathbf{a}(\theta_0)|^2} = \frac{\left| \frac{\mathbf{w}_{k-1}^H \mathbf{a}(\theta_k)\mathbf{a}^H(\theta_k)}{\mathbf{a}^H(\theta_k)\mathbf{a}(\theta_k)} \mathbf{a}(\theta_k) \right|^2}{\left| \frac{\mathbf{w}_{k-1}^H \mathbf{a}(\theta_k)\mathbf{a}^H(\theta_k)}{\mathbf{a}^H(\theta_k)\mathbf{a}(\theta_k)} \mathbf{a}(\theta_0) \right|^2} = \tilde{\rho}_k. \quad (76)$$

Clearly, if  $\rho_k < \tilde{\rho}_k$ , it is readily known that (73) holds true.

Now recalling the expression of  $\mathbf{c}_{\beta_k}$  in (17), and combining the conclusions of *Step 1* and *Step 2*, one obtains that

$$\mathbf{c}_{\beta_k}(2) = 0 \quad \text{and} \quad \mathbf{c}_{\beta_k}(1) \geq 0 \quad (77)$$

provided that  $\mathbf{w}_{k-1} = \mathbf{a}(\theta_0)$  and  $0 \leq \rho_k < \tilde{\rho}_k$ .

*Step 3:* In the third step, we will show that

$$\mathbf{c}_{\beta_k}(1) \leq 1 \quad (78)$$

provided that  $\mathbf{w}_{k-1} = \mathbf{a}(\theta_0)$ ,  $0 \leq \rho_k \leq \min\{\tilde{\rho}_k, \bar{\rho}_k\}$  and  $\rho_k \neq \tilde{\rho}_k$ .

To do so, we first note that  $\rho_k < \tilde{\rho}_k$  indicates  $\mathbf{B}_k(2, 2) > 0$ . Then,  $\mathbf{c}_{\beta_k}(1) \leq 1$  can be rewritten as

$$-\Re(\mathbf{B}_k(1, 2)) = -\mathbf{B}_k(1, 2) \leq \mathbf{B}_k(2, 2) \quad (79)$$

where  $\mathbf{B}_k(1, 2) \in \mathbb{R}$  has been utilized. Recalling (70) and the expression of  $\mathbf{B}_k(2, 2)$ , one can reshape (79) as

$$\rho_k \mathbf{w}_{k-1}^H \mathbf{a}(\theta_0)\mathbf{a}^H(\theta_0)\mathbf{w}_{\parallel} \leq |\mathbf{w}_{\parallel}^H \mathbf{a}(\theta_k)|^2 \quad (80)$$

and further

$$\frac{\rho_k \|\mathbf{a}(\theta_0)\|_2^2 \cdot |\mathbf{a}^H(\theta_0)\mathbf{a}(\theta_k)|^2}{\|\mathbf{a}(\theta_k)\|_2^2} \leq |\mathbf{a}^H(\theta_0)\mathbf{a}(\theta_k)|^2. \quad (81)$$

In fact, (81) can be reformulated as  $\rho_k \leq \bar{\rho}_k$ . As a consequence, we learn that  $\mathbf{c}_{\beta_k}(1) \leq 1$ , provided that  $\mathbf{w}_{k-1} = \mathbf{a}(\theta_0)$ ,  $0 \leq \rho_k \leq \min\{\tilde{\rho}_k, \bar{\rho}_k\}$  and  $\rho_k \neq \tilde{\rho}_k$ .

Recalling (77), it can be summarized that  $\mathbf{c}_{\beta_k}(2) = 0$  and  $\mathbf{c}_{\beta_k}(1) \in [0, 1]$ , provided that  $\mathbf{w}_{k-1} = \mathbf{a}(\theta_0)$ ,  $0 \leq \rho_k \leq \min\{\tilde{\rho}_k, \bar{\rho}_k\}$  and  $\rho_k \neq \tilde{\rho}_k$ . According to Proposition 4, we have  $T(\beta_{k,\star}) = \mu_{k,s} = \mu_{k,\star}$ , which implies that  $\mathbf{C}^2$ -WORD obtains the same weight vector  $\mathbf{w}_k$  as  $\mathbf{A}^2\mathbf{RC}$ . This completes the proof.

## APPENDIX G PROOF OF COROLLARY 2

Before the proof, we give the following property **P** about set  $\mathbb{V}$ , which is useful in the later derivations.

$$\boxed{\mathbf{P}: \text{For } \forall \mathbf{v}_1, \mathbf{v}_2 \in \mathbb{V}, \forall c_1, c_2 \in \mathbb{R}, \text{ we have } c_1 \mathbf{v}_1 + c_2 \mathbf{v}_2 \in \mathbb{V}.}$$

The above property **P** can be readily proofed from the definition of set  $\mathbb{V}$ , we omit the details for space limitation.

Then, it requires three steps to complete the proof of Corollary 2.

*Step 1:* In the first step, we will proof that

$$\Im(\mathbf{v}_1^H \mathbf{v}_2) = 0, \quad \forall \mathbf{v}_1, \mathbf{v}_2 \in \mathbb{V}. \quad (82)$$

Without loss of generality, we assume that  $N$  is even, the case that  $N$  is odd is similar. Then for  $\forall \mathbf{v} \in \mathbb{V}$ , we denote an associated vector  $\mathbf{d}$  by

$$\mathbf{d} \triangleq [\mathbf{v}(1) \quad \mathbf{v}(2) \quad \cdots \quad \mathbf{v}(N/2)]^T. \quad (83)$$

Recalling the definition of set  $\mathbb{V}$ , we know that

$$\begin{bmatrix} \Re(\mathbf{v}) \\ \Im(\mathbf{v}) \end{bmatrix} = \mathbf{G}_1 \begin{bmatrix} \Re(\mathbf{d}) \\ \Im(\mathbf{d}) \end{bmatrix}, \quad \begin{bmatrix} \Im(\mathbf{v}) \\ -\Re(\mathbf{v}) \end{bmatrix} = \mathbf{G}_2 \begin{bmatrix} \Re(\mathbf{d}) \\ \Im(\mathbf{d}) \end{bmatrix} \quad (84)$$

where  $\mathbf{G}_1$  and  $\mathbf{G}_2$  are defined as

$$\mathbf{G}_1 \triangleq \begin{bmatrix} \mathbf{I} & \mathbf{0} \\ \mathbf{J} & \mathbf{0} \\ \mathbf{0} & \mathbf{I} \\ \mathbf{0} & -\mathbf{J} \end{bmatrix}, \quad \mathbf{G}_2 \triangleq \begin{bmatrix} \mathbf{0} & \mathbf{I} \\ \mathbf{0} & -\mathbf{J} \\ -\mathbf{I} & \mathbf{0} \\ -\mathbf{J} & \mathbf{0} \end{bmatrix} \quad (85)$$

with  $\mathbf{I}$  standing for the  $N/2$ -dimensional identity matrix,  $\mathbf{J}$  denoting the  $N/2$ -dimensional exchange matrix with ones on its anti-diagonal and zeros elsewhere. It can be validated that  $\mathbf{G}_1^T \mathbf{G}_2 = \mathbf{0}$ . Then for  $\forall \mathbf{v}_1, \mathbf{v}_2 \in \mathbb{V}$ , we have

$$\Im(\mathbf{v}_1^H \mathbf{v}_2) = [\Re(\mathbf{d}_1^T) \quad \Im(\mathbf{d}_1^T)] \mathbf{G}_1^T \mathbf{G}_2 \begin{bmatrix} \Re(\mathbf{d}_2) \\ \Im(\mathbf{d}_2) \end{bmatrix} = 0 \quad (86)$$

where  $\mathbf{d}_1$  and  $\mathbf{d}_2$  stand for the associated vectors of  $\mathbf{v}_1$  and  $\mathbf{v}_2$ , respectively. This completes the proof of (82).

*Step 2:* In this step, it is necessary to show that if  $0 \leq \rho_k < \tilde{\rho}_k$ , then  $\mathbf{B}_k(2, 2) > 0$ . See *Step 2* in the derivation of Corollary 1 for details.

*Step 3:* In this step, we first assume that  $\mathbf{w}_{k-1} \in \mathbb{V}$ . Then considering the centro-symmetric arrays (both  $\mathbf{a}(\theta_0)$  and  $\mathbf{a}(\theta_k)$  are in set  $\mathbb{V}$ ), we have  $\mathbf{a}^H(\theta_k)\mathbf{w}_{k-1} \in \mathbb{R}$ . Recalling the property **P**, one obtains  $\mathbf{w}_{\parallel} = \mathbf{a}(\theta_k)\mathbf{a}^H(\theta_k)\mathbf{w}_{k-1}/\|\mathbf{a}(\theta_k)\|_2^2 \in \mathbb{V}$  and  $\mathbf{w}_{\perp} = \mathbf{w}_{k-1} - \mathbf{w}_{\parallel} \in \mathbb{V}$ . Therefore, we have  $\Im(\mathbf{w}_{\perp}^H \mathbf{a}(\theta_0)\mathbf{a}^H(\theta_0)\mathbf{w}_{\parallel}) = 0$  and

$$\begin{aligned} \mathbf{c}_{\beta_k}(2) &= \Im(\mathbf{B}_k(1, 2))/\mathbf{B}_k(2, 2) \\ &= -\rho_k \Im(\mathbf{w}_{\perp}^H \mathbf{a}(\theta_0)\mathbf{a}^H(\theta_0)\mathbf{w}_{\parallel})/\mathbf{B}_k(2, 2) = 0. \end{aligned} \quad (87)$$

Combining the result of *Step 2* (more exactly, inequity (73)), we have

$$\begin{aligned} \mathbf{c}_{\beta_k}(1) &= -\Re(\mathbf{B}_k(1, 2))/\mathbf{B}_k(2, 2) \\ &= \rho_k \mathbf{w}_{\perp}^H \mathbf{a}(\theta_0)\mathbf{a}^H(\theta_0)\mathbf{w}_{\parallel}/\mathbf{B}_k(2, 2) \geq 0 \end{aligned} \quad (88)$$

provided that  $\mathbf{w}_{\perp}^H \mathbf{a}(\theta_0)\mathbf{a}^H(\theta_0)\mathbf{w}_{\parallel} \geq 0$  and  $0 \leq \rho_k \leq \tilde{\rho}_k$ .

Also, it can be observed from  $\mathbf{w}_{\perp}^H \mathbf{a}(\theta_0)\mathbf{a}^H(\theta_0)\mathbf{w}_{\parallel} \geq 0$  that  $\mathbf{w}_{k-1}^H \mathbf{a}(\theta_0)\mathbf{a}^H(\theta_0)\mathbf{w}_{\parallel} \geq \mathbf{w}_{\parallel}^H \mathbf{a}(\theta_0)\mathbf{a}^H(\theta_0)\mathbf{w}_{\parallel}$ , and further

$$\begin{aligned} &\frac{\mathbf{w}_{k-1}^H \mathbf{a}(\theta_0)\mathbf{a}^H(\theta_0)\mathbf{a}(\theta_k)\mathbf{a}^H(\theta_k)\mathbf{w}_{k-1}}{\mathbf{a}^H(\theta_k)\mathbf{a}(\theta_k)} \\ &= \mathbf{w}_{k-1}^H \mathbf{a}(\theta_0)\mathbf{a}^H(\theta_0)\mathbf{w}_{\parallel} \geq \mathbf{w}_{\parallel}^H \mathbf{a}(\theta_0)\mathbf{a}^H(\theta_0)\mathbf{w}_{\parallel} \geq 0. \end{aligned} \quad (89)$$

On this basis, if  $\mathbf{w}_{\perp}^H \mathbf{a}(\theta_0)\mathbf{a}^H(\theta_0)\mathbf{w}_{\parallel} \geq 0$ , we have

$$\frac{\mathbf{w}_{k-1}^H \mathbf{a}(\theta_k)\mathbf{a}^H(\theta_k)\mathbf{a}(\theta_k)\mathbf{a}^H(\theta_k)\mathbf{w}_{k-1}}{\mathbf{w}_{k-1}^H \mathbf{a}(\theta_0)\mathbf{a}^H(\theta_0)\mathbf{a}(\theta_k)\mathbf{a}^H(\theta_k)\mathbf{w}_{k-1}} = \check{\rho}_k \quad (90)$$

where  $\check{\rho}_k$  has been defined in (30b). If  $\rho_k \leq \check{\rho}_k$  is satisfied, then from (89), (90) and the expression of  $\mathbf{w}_{\parallel}$  in (75), we obtain

$$\rho_k \mathbf{w}_{\perp}^H \mathbf{a}(\theta_0)\mathbf{a}^H(\theta_0)\mathbf{w}_{\parallel} \leq \mathbf{w}_{\parallel}^H \mathbf{a}(\theta_k)\mathbf{a}^H(\theta_k)\mathbf{w}_{\parallel} \quad (91)$$

which can be reformulated as  $0 \leq \rho_k \mathbf{w}_\perp^H \mathbf{a}(\theta_0) \mathbf{a}^H(\theta_0) \mathbf{w}_\parallel \leq |\mathbf{w}_\parallel^H \mathbf{a}(\theta_k)|^2 - \rho_k |\mathbf{w}_\parallel^H \mathbf{a}(\theta_0)|^2$ , or simply  $0 \leq -\Re(\mathbf{B}_k(1, 2)) \leq \mathbf{B}_k(2, 2)$ . As a result, one gets

$$\mathbf{c}_{\beta_k}(1) = -\Re(\mathbf{B}_k(1, 2))/\mathbf{B}_k(2, 2) \leq 1. \quad (92)$$

Then we can summarize that for a centro-symmetric array, if  $\mathbf{w}_{k-1} \in \mathbb{V}$ ,  $0 \leq \rho_k \leq \min\{\tilde{\rho}_k, \check{\rho}_k\}$ ,  $\rho_k \neq \tilde{\rho}_k$  and  $\mathbf{w}_\perp^H \mathbf{a}(\theta_0) \mathbf{a}^H(\theta_0) \mathbf{w}_\parallel \geq 0$ , then  $\mathbf{c}_{\beta_k}(2) = 0$  and  $\mathbf{c}_{\beta_k}(1) \in [0, 1]$ . Recalling Proposition 4, we have  $T(\beta_{k,*}) = \mu_{k,*}$  and  $\beta_{k,*} \in \mathbb{R}$ . Thus, an identical weight vector  $\mathbf{w}_k$  will be resulted by  $\mathbf{C}^2$ -WORD and  $\mathbf{A}^2\mathbf{RC}$  in the  $k$ th response control step. More importantly, we have  $\mathbf{w}_k = \mathbf{w}_\perp + \beta_{k,*} \mathbf{w}_\parallel \in \mathbb{V}$ . Consequently, it can be recursive out  $\mathbf{w}_k \in \mathbb{V}$  and  $T(\beta_{k+1,*}) = \mu_{k+1,*}$ , provided that  $\mathbf{w}_{k-1} \in \mathbb{V}$ , and both (19) and (30b) are satisfied. Then obviously, if  $\mathbf{w}_0 \in \mathbb{V}$ , we can infer that  $T(\beta_{k,*}) = \mu_{k,*}$  (i.e.,  $\mathbf{C}^2$ -WORD becomes equivalent to  $\mathbf{A}^2\mathbf{RC}$ ) for  $k = 1, 2, \dots$ , as long as (19) and (30b) hold true for every subscript  $k$ . This completes the proof.

## REFERENCES

- [1] M. H. Er, "Array pattern synthesis with a controlled mean-square sidelobe level," *IEEE Trans. Signal Process.*, vol. 40, no. 4, pp. 977–981, 1992.
- [2] B. Fuchs and S. Rondineau, "Array pattern synthesis with excitation control via norm minimization," *IEEE Trans. Antennas Propag.*, vol. 64, pp. 4228–4234, 2016.
- [3] B. Fuchs and J. J. Fuchs, "Optimal narrow beam low sidelobe synthesis for arbitrary arrays," *IEEE Trans. Antennas Propag.*, vol. 58, pp. 2130–2135, 2010.
- [4] G. Oliveri, M. Salucci, and A. Massa, "Synthesis of modular contiguously clustered linear arrays through a sparseness-regularized solver," *IEEE Trans. Antennas Propag.*, vol. 64, pp. 4277–4287, 2016.
- [5] C. Y. Tseng and L. J. Griffiths, "A simple algorithm to achieve desired patterns for arbitrary arrays," *IEEE Trans. Signal Process.*, vol. 40, pp. 2737–2746, 1992.
- [6] C. L. Dolph, "A current distribution for broadside arrays which optimizes the relationship between beam width and side-lobe level," *Proc. IRE*, vol. 34, pp. 335–348, 1946.
- [7] K. K. Yan and Y. Lu, "Sidelobe reduction in array-pattern synthesis using genetic algorithm," *IEEE Trans. Antennas Propag.*, vol. 45, pp. 1117–1122, 1997.
- [8] D. W. Boeringer and D. H. Werner, "Particle swarm optimization versus genetic algorithms for phased array synthesis," *IEEE Trans. Antennas Propag.*, vol. 52, pp. 771–779, 2004.
- [9] V. Murino, A. Trucco, and C. S. Regazzoni, "Synthesis of unequally spaced arrays by simulated annealing," *IEEE Trans. Signal Process.*, vol. 44, pp. 119–122, 1996.
- [10] H. L. Van Trees, *Optimum Array Processing*. New York: Wiley, 2002.
- [11] C. A. Olen and R. T. Compton, "A numerical pattern synthesis algorithm for arrays," *IEEE Trans. Antennas Propag.*, vol. 38, pp. 1666–1676, 1990.
- [12] W. A. Swart and J. C. Olivier, "Numerical synthesis of arbitrary discrete arrays," *IEEE Trans. Antennas Propag.*, vol. 41, pp. 1171–1174, 1993.
- [13] P. Y. Zhou and M. A. Ingram, "Pattern synthesis for arbitrary arrays using an adaptive array method," *IEEE Trans. Antennas Propag.*, vol. 47, pp. 862–869, 1999.
- [14] S. Boyd and L. Vandenberghe, *Convex Optimization*. Cambridge, U.K.: Cambridge Univ. Press, 2004.
- [15] P. J. Kajenski, "Phase only antenna pattern notching via a semidefinite programming relaxation," *IEEE Trans. Antennas Propag.*, vol. 60, pp. 2562–2565, 2012.
- [16] P. Rocca, N. Anselmi, and A. Massa, "Optimal synthesis of robust beam-former weights exploiting interval analysis and convex optimization," *IEEE Trans. Antennas Propag.*, vol. 62, pp. 3603–3612, 2014.
- [17] G. Oliveri, L. Poli, and A. Massa, "Maximum efficiency beam synthesis of radiating planar arrays for wireless power transmission," *IEEE Trans. Antennas Propag.*, vol. 61, pp. 2490–2499, 2013.
- [18] H. Lebreton and S. Boyd, "Antenna array pattern synthesis via convex optimization," *IEEE Trans. Signal Process.*, vol. 45, pp. 526–532, 1997.
- [19] H. G. Hoang, H. D. Tuan, and B. N. Vo, "Low-dimensional SDP formulation for large antenna array synthesis," *IEEE Trans. Antennas Propag.*, vol. 55, pp. 1716–1725, 2007.
- [20] F. Wang, V. Balakrishnan, P. Y. Zhou, J. J. Chen, R. Yang, and C. Frank, "Optimal array pattern synthesis using semidefinite programming," *IEEE Trans. Signal Process.*, vol. 51, pp. 1172–1183, 2003.
- [21] K. M. Tsui and S. C. Chan, "Pattern synthesis of narrowband conformal arrays using iterative second-order cone programming," *IEEE Trans. Antennas Propag.*, vol. 58, no. 6, pp. 1959–1970, 2010.
- [22] S. E. Nai, W. Ser, Z. L. Yu, and H. Chen, "Beampattern synthesis for linear and planar arrays with antenna selection by convex optimization," *IEEE Trans. Antennas Propag.*, vol. 58, pp. 3923–3930, 2010.
- [23] B. Fuchs, "Application of convex relaxation to array synthesis problems," *IEEE Trans. Antennas Propag.*, vol. 62, pp. 634–640, 2014.
- [24] Z.-Q. Luo, W.-K. Ma, A. M.-C. So, Y. Ye, and S. Zhang, "Semidefinite relaxation of quadratic optimization problems," *IEEE Signal Process. Mag.*, vol. 27, pp. 20–34, 2010.
- [25] F. Wang, R. Yang, and C. Frank, "A new algorithm for array pattern synthesis using the recursive least squares method," *IEEE Signal Process. Lett.*, vol. 10, pp. 235–238, 2003.
- [26] K. Yang, Z. Zhao, Z. Nie, J. Ouyang, and Q. H. Liu, "Synthesis of conformal phased arrays with embedded element pattern decomposition," *IEEE Trans. Antennas Propag.*, vol. 59, pp. 2882–2888, 2011.
- [27] L. Manica, P. Rocca, and A. Massa, "Design of subarrayed linear and planar array antennas with SLL control based on an excitation matching approach," *IEEE Trans. Antennas Propag.*, vol. 57, pp. 1684–1691, 2009.
- [28] X. Zhang, Z. He, B. Liao, X. Zhang, Z. Cheng, and Y. Lu, " $\mathbf{A}^2\mathbf{RC}$ : an accurate array response control algorithm for pattern synthesis," *IEEE Trans. Signal Process.*, vol. 65, pp. 1810–1824, 2017.
- [29] X. Zhang, Z. He, B. Liao, X. Zhang, and W. Peng, "Pattern synthesis for arbitrary arrays via weight vector orthogonal decomposition," *IEEE Trans. Signal Process.*, vol. 66, pp. 1286–1299, 2018.
- [30] R. C. Nongpiur and D. J. Shpak, "Synthesis of linear and planar arrays with minimum element selection," *IEEE Trans. Signal Process.*, vol. 62, pp. 5398–5410, 2014.
- [31] H. Cox, R. M. Zeskind, and M. M. Owen, "Robust adaptive beam-forming," *IEEE Trans. Acoust., Speech, Signal Process.*, vol. 35, pp. 1365–1376, 1987.
- [32] H. Cox, R. Zeskind, and T. Kooij, "Practical supergain," *IEEE Trans. Acoust., Speech, Signal Process.*, vol. 34, pp. 393–398, 1986.
- [33] X. Zhang, Z. He, and X. Zhang, "Pattern synthesis via complex-coefficient weight vector orthogonal decomposition—Part II: Robust sidelobe synthesis," preprint, Aug. 2018.
- [34] G. H. Golub and C. F. V. Loan, *Matrix Computations*. Baltimore, MD: The Johns Hopkins Univ. Press, 1996.
- [35] G. Xu, R. H. Roy, and T. Kailath, "Detection of number of sources via exploitation of centro-symmetry property," *IEEE Trans. Signal Process.*, vol. 42, pp. 102–112, 1994.
- [36] M. Haardt and J. A. Nosske, "Unitary ESPRIT: how to obtain increased estimation accuracy with a reduced computational burden," *IEEE Trans. Signal Process.*, vol. 43, pp. 1232–1242, 1995.
- [37] J. Steinwandt, F. Roemer, M. Haardt, and G. D. Galdo, "R-dimensional ESPRIT-type algorithms for strictly second-order non-circular sources and their performance analysis," *IEEE Trans. Signal Process.*, vol. 62, pp. 4824–4838, 2014.
- [38] C. M. Schmid, S. Schuster, R. Feger, and A. Stelzer, "On the effects of calibration errors and mutual coupling on the beam pattern of an antenna array," *IEEE Trans. Antennas Propag.*, vol. 61, no. 8, pp. 4063–4072, 2013.
- [39] X. Zhang, Z. He, B. Liao, X. Zhang, and W. Peng, "Pattern synthesis with multipoint accurate array response control," *IEEE Trans. Antennas Propag.*, vol. 65, pp. 4075–4088, 2017.
- [40] L. I. Vaskelainen, "Iterative least-squares synthesis methods for conformal array antennas with optimized polarization and frequency properties," *IEEE Trans. Antennas Propag.*, vol. 45, no. 7, pp. 1179–1185, 1997.
- [41] L. Zou, J. Lasenby, and Z. He, "Direction and polarization estimation using polarized cylindrical conformal arrays," *IET Signal Process.*, vol. 6, no. 5, pp. 395–403, 2012.
- [42] B. H. Wang, Y. Guo, Y. L. Wang, and Y. Z. Lin, "Frequency-invariant pattern synthesis of conformal array antenna with low cross-polarization," *IET Microw. Antennas Propag.*, vol. 2, no. 5, pp. 442–450, 2008.
- [43] B. Fuchs and J. J. Fuchs, "Optimal polarization synthesis of arbitrary arrays with focused power pattern," *IEEE Trans. Antennas Propag.*, vol. 59, no. 12, pp. 4512–4519, 2011.